

## Point-by-point response to referee comments

### Response to reviewers

Key:

- Reviewers' comments
- Author's response
- Modified text in the manuscript

Editor Decision:

Comments to the Author:

Dear Jianjun Zou,

I have now received feedback from the two reviewers on your revised manuscript "Millennial-scale variations of sedimentary oxygenation in the western subtropical North Pacific and its links to the North Atlantic climate" submitted to *Climate of the Past*. Both reviewers are very pleased with the way you addressed and responded to their comments given in the first round of reviews, and recommend to accept the paper after technical corrections. I will therefore ask you to respond to the minor comments raised in the new reviewer reports before final acceptance of the paper.

Best regards,

Björg Risebrobakken

Editor, *Climate of the Past*

Reply#1: We thank both reviewers for commenting positively on the revised version of our original manuscript. We particularly appreciate that each reviewer found that our manuscript is worth for publication after minor technical corrections.

Referee #1

Zou et al have made substantial revision to their manuscript 'Millennial-scale variations of sedimentary oxygenation in the western subtropical North Pacific and its links to North Atlantic climate'.

I only have a few (small) comments, and I am happy to see the manuscript published once these have been considered:

Abstract:

Lines 36-38: the way I read this is that an increase in deep ocean respired CO<sub>2</sub>

concentrations leads to deoxygenation of the upper water column (e.g. top 1000 m represents subsurface layer). Subsurface is not necessarily the same as mid-depth, which I think is what you actually mean? Perhaps remnant of (copied and pasted from response reviewers comments):

‘Lines 848-846 (484-486? ) : does not make sense. How does subsurface water oxygen consumption lead to lower oxygen concentrations in deeper waters?’

Reply#30: Thanks for your suggestion. We have removed the sentence in the revised manuscript. The replenishment of oxygen in deep water is controlled by both lateral advection and vertical supply. The oxygen consumption in subsurface water would reduce the oxygen content in the ocean interior, thus lead to a lower oxygen concentration in deeper waters.’

Reply#2: Thanks for this comment. Here we would like to highlight the deoxygenation in the ocean interior at that time. In order to make a clear statement, the subsurface was replaced by **ocean interior** in Line 38 of the revised manuscript.

As stated in Reply#30 of the first-round of response letter, we suggested the oxygen consumption because of organic matter degradation in the ocean interior would reduce the vertical supply of oxygen to deeper waters, despite the replenishment of oxygen due to lateral advection.

Lines 45 to 48: perhaps rephrase; e.g. cold spells enhanced oxygenation linked to NPIW, while interglacial increase after 8.5 ka linked to intensification of Kuroshio Current.

Add a line about why the Kuroshio Current intensified?

Reply#3: Thanks. We rephrased this sentence as follows. Please refer to Lines 45-48 in the revised MS.

“The enhanced oxygenation during cold spells is linked to the North Pacific Intermediate Water (NPIW), while interglacial increase after 8.5 ka is linked to an intensification of the Kuroshio Current due to strengthened northeast trade winds over the tropics.”

Line 62: add 'is' between pump and widely.

Reply#4: Added in Line 62 of the revised manuscript.

Introduction:

Lines 88-89: do you mean a small subpolar input or a minimum input, or reducing the input (as it read now)?

Reply#5: Thanks. The word lower was replaced by **small** in Line 88 of the revised manuscript.

Material and methods: could you add the response to this query to the section? Gives strength to your interpretation.

Reply#6: Thanks. We agree with this suggestion. In the revised manuscript (Lines 281-285), the following sentence (including references) has been added to give more information on sedimentation rate.

“Variation in sedimentation rate has been attributed to changes in eustatic sea level, summer EAM intensity, path and/or intensity of Kuroshio Current. Generally, sea level is thought to be the first-order factor for controlling linear sedimentation rate changes (Beny et al., 2018; Li et al., 2015; Zhao et al., 2017).”

Anonymous Referee #2

The authors have substantially revised their manuscript, which I feel now has the attributes to be accepted for publication in *Climate of the Past*. I appreciate the thoroughness of their rebuttal letter, well done!

I have two last very minor comments, which I would like to see addressed before the manuscript can be formally accepted -

1. 311 and throughout – I’m not sure I understand why Mn is plotted as total Mn and not, like U and Mo, as Mn<sub>excess</sub> or Mn/Al for example?

Reply#7: In this study, the Mo/Mn ratio is a ratio of total Mo concentration to total Mn concentration. The main reasons that the Mo/Mn ratio was used are ascribed to (1) the contrasting geochemical behaviors between these two elements and (2) a strong positive correlation between Mo/Mn and excess U.

The sedimentary Mn concentration in core CSH1 ranges between 0.04% and 0.06% with an average of 0.05% over the last 50ka, which is less than the Mn concentrations in Upper Crust (0.06%) (Taylor and McLennan, 2009), the suspended particulate matter of Yangtze River (0.116%) (Gaillardet et al., 1999) and the average shale (0.085%) (Li and Schoonmaker, 2014). Therefore, there is no excess Mn in sediments of core CSH1. The reason can be ascribed to dilution by biogenic materials and dissolution of Mn oxides and oxyhydroxides.

We also calculated the ratio of Mn/Al and it shows a similar downcore trend to that of total Mn concentration (Figure S1) and therefore we preferred the total Mn rather than Mn/Al ratio in the manuscript.

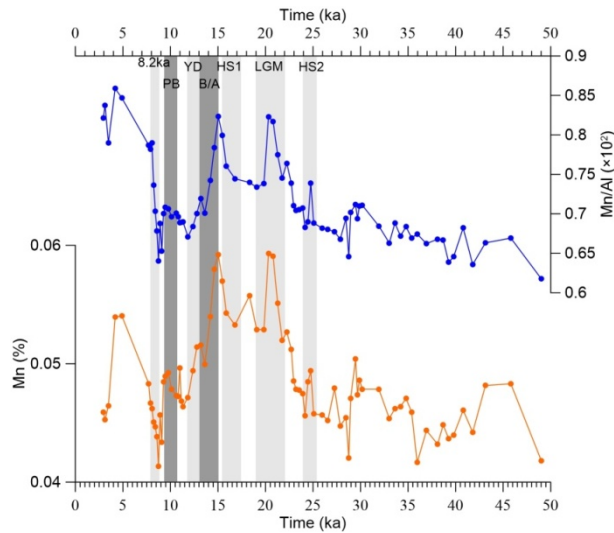


Figure S1 Downcore records of Mn concentration and Mn/Al ratio in core CSH1 over the last 50 ka.

Fig. 7, pannel d, the Pa/Th record has superposed measurements, which I think must be a small mistake.

Reply#8: In Fig.7d, the data of Pa/Th are taken from two references (Böhm et al., 2015; McManus et al., 2004). In order to make distinction of these two sources, different colored lines are used in revised Figure 7d.

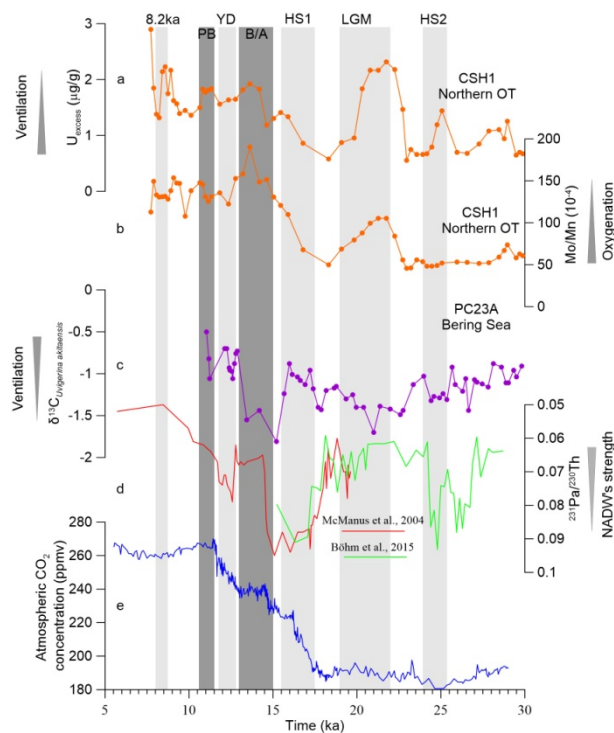


Figure 7. Proxy records favoring the existence of out-of-phase connections between

the subtropical North Pacific and North Atlantic during the last deglaciation and enhanced carbon storage at mid-depth waters. (a)  $U_{\text{excess}}$  concentration in core CSH1; (b) Mo/Mn ratio in core CSH1; (c) benthic  $\delta^{13}\text{C}$  record in core PC-23A in the Bering Sea (Rella et al., 2012); (d) Indicator of strength of Atlantic Meridional Ocean Circulation ( $^{231}\text{Pa}/^{230}\text{Th}$ ) (Böhm et al., 2015; McManus et al., 2004); (e) Atmospheric  $\text{CO}_2$  concentration (Marcott et al., 2014). Light gray and dark gray vertical bars are the same as those in Figure 4.

## References

- Böhm, E., Lippold, J., Gutjahr, M., Frank, M., Blaser, P., Antz, B., Fohlmeister, J., Frank, N., Andersen, M. B., and Deininger, M.: Strong and deep Atlantic meridional overturning circulation during the last glacial cycle, *Nature*, 517, 73-76, 2015.
- Beny, F., Toucanne, S., Skonieczny, C., Bayon, G., and Ziegler, M.: Geochemical provenance of sediments from the northern East China Sea document a gradual migration of the Asian Monsoon belt over the past 400,000 years, *Quaternary Science Reviews*, 190, 161-175, 2018.
- Gaillardet, J., Dupré, B., and Allègre, C. J.: Geochemistry of large river suspended sediments: silicate weathering or recycling tracer?, *Geochimica et Cosmochimica Acta*, 63, 4037-4051, 1999.
- Li, T., Xu, Z., Lim, D., Chang, F., Wan, S., Jung, H., and Choi, J.: Sr-Nd isotopic constraints on detrital sediment provenance and paleoenvironmental change in the northern Okinawa Trough during the late Quaternary, *Palaeogeography, Palaeoclimatology, Palaeoecology*, 430, 74-84, 2015.
- Li, Y. H. and Schoonmaker, J. E.: Chemical Composition and Mineralogy of Marine Sediments. In: *Treatise on Geochemistry (Second Edition)*, Holland, H. D. and Turekian, K. K. (Eds.), Elsevier, Oxford, 2014.
- Marcott, S. A., Bauska, T. K., Buizert, C., Steig, E. J., Rosen, J. L., Cuffey, K. M., Fudge, T. J., Severinghaus, J. P., Ahn, J., Kalk, M. L., McConnell, J. R., Sowers, T., Taylor, K. C., White, J. W. C., and Brook, E. J.: Centennial-scale changes in the global carbon cycle during the last deglaciation, *Nature*, 514, 616-619, 2014.
- McManus, J. F., Francois, R., Gherardi, J. M., Keigwin, L. D., and Brown-Leger, S.: Collapse and rapid resumption of Atlantic meridional circulation linked to deglacial climate changes, *Nature*, 428, 834-837, 2004.
- Rella, S. F., Tada, R., Nagashima, K., Ikehara, M., Itaki, T., Ohkushi, K., Sakamoto, T., Harada, N., and Uchida, M.: Abrupt changes of intermediate water properties on the northeastern slope of the Bering Sea during the last glacial and deglacial period, *Paleoceanography*, 27, PA3203, doi:3210.1029/2011pa002205, 2012.
- Taylor, S. R. and McLennan, S.: *Planetary Crusts: Their Composition, Origin and Evolution*, Cambridge University Press, Cambridge, 2009.
- Zhao, D., Wan, S., Toucanne, S., Clift, P. D., Tada, R., Révillon, S., Kubota, Y., Zheng, X., Yu, Z., Huang, J., Jiang, H., Xu, Z., Shi, X., and Li, A.: Distinct control mechanism of fine-grained sediments from Yellow River and Kyushu supply in the northern Okinawa Trough since the last glacial, *Geochemistry, Geophysics, Geosystems*, 18, 2949-2969, 2017.

1 **Millennial-scale variations of sedimentary oxygenation in the western**  
2 **subtropical North Pacific and its links to North Atlantic climate**

3  
4 Jianjun Zou<sup>1,2</sup>, Xuefa Shi<sup>1,2</sup>, Aimei Zhu<sup>1</sup>, Selvaraj Kandasamy<sup>3</sup>, Xun Gong<sup>4</sup>, Lester  
5 Lembke-Jene<sup>4</sup>, Min-Te Chen<sup>5</sup>, Yonghua Wu<sup>1,2</sup>, Shulan Ge<sup>1,2</sup>, Yanguang Liu<sup>1,2</sup>, Xinru  
6 Xue<sup>1</sup>, Gerrit Lohmann<sup>4</sup>, Ralf Tiedemann<sup>4</sup>

7 <sup>1</sup>Key Laboratory of Marine Sedimentology and Environmental Geology, First Institute  
8 of Oceanography, MNR, Qingdao 266061, China

9 <sup>2</sup>Laboratory for Marine Geology, Qingdao National Laboratory for Marine Science  
10 and Technology, Qingdao, 266061, China

11 <sup>3</sup>Department of Geological Oceanography and State Key Laboratory of Marine  
12 Environmental Science, Xiamen University, Xiamen361102, China

13 <sup>4</sup>Alfred-Wegener-Institut Helmholtz-Zentrum für Polar- und Meeresforschung, Am  
14 Handelshafen 12, 27570 Bremerhaven, Germany

15 <sup>5</sup>Institute of Applied Geosciences, National Taiwan Ocean University, Keelung 20224,  
16 Taiwan

17  
18 Corresponding authors:

19 Jianjun Zou ([zoujianjun@fio.org.cn](mailto:zoujianjun@fio.org.cn)); Xuefa Shi ([xfshi@fio.org.cn](mailto:xfshi@fio.org.cn))

20 **Key Points**

21 1. This study reconstructs the history of sedimentary oxygenation processes at  
22 mid-depths in the western subtropical North Pacific since the last glacial period.

23 2. Sediment-bound redox-sensitive proxies reveal millennial-scale variations in  
24 sedimentary oxygenation that correlated closely to changes in the North Pacific  
25 Intermediate Water.

26 3. A millennial-scale out-of-phase relationship between deglacial ventilation in the  
27 western subtropical North Pacific and the formation of North Atlantic Deep Water is  
28 suggested.

29 4. A larger CO<sub>2</sub> storage at mid-depths of the North Pacific corresponds to the  
30 termination of atmospheric CO<sub>2</sub> rise during the Bölling-Alleröd interval.

31 **Abstract**

32 The deep ocean carbon cycle, especially carbon sequestration and outgassing, is  
33 one of the mechanisms to explain variations in atmospheric CO<sub>2</sub> concentrations on  
34 millennial and orbital timescales. However, the potential role of subtropical North  
35 Pacific subsurface waters in modulating atmospheric CO<sub>2</sub> levels on millennial  
36 timescales is poorly constrained. An increase in respired CO<sub>2</sub> concentration in the  
37 glacial deep ocean due to biological pump generally corresponds to deoxygenation in  
38 the ~~subsurface layer~~ocean interior. This link thus offers a chance to study oceanic  
39 ventilation and coeval export productivity based on redox-controlled, sedimentary  
40 geochemical parameters. Here, we investigate a suite of geochemical proxies in a  
41 sediment core from the Okinawa Trough to understand sedimentary oxygenation  
42 variations in the subtropical North Pacific over the last 50,000 years (50 ka). Our  
43 results suggest that enhanced mid-depth western subtropical North Pacific (WSTNP)  
44 sedimentary oxygenation occurred during cold intervals and after 8.5 ka, while  
45 oxygenation decreased during the Bölling-Alleröd (B/A) and Preboreal. ~~The enhanced~~  
46 ~~oxygenation during cold spells is linked to the North Pacific Intermediate Water~~  
47 ~~(NPIW), while interglacial increase after 8.5 ka is linked to an intensification of the~~  
48 ~~Kuroshio Current due to strengthened northeast trade winds over the tropics. The~~  
49 ~~enhanced sedimentary oxygenation in the WSTNP is aligned with intensified~~  
50 ~~formation of North Pacific Intermediate Water (NPIW) during cold spells, while better~~  
51 ~~sedimentary oxygenation seems to be linked to an intensified Kuroshio Current after~~  
52 ~~8.5 ka.~~The enhanced formation of NPIW during Heinrich Stadial 1 (HS1) was likely  
53 driven by the perturbation of sea ice formation and sea surface salinity oscillations in  
54 high-latitude North Pacific. The diminished sedimentary oxygenation during the B/A  
55 due to decreased NPIW formation and enhanced export production, indicates an  
56 expansion of oxygen minimum zone in the North Pacific and enhanced CO<sub>2</sub>  
57 sequestration at mid-depth waters, along with termination of atmospheric CO<sub>2</sub>  
58 concentration increase. We attribute the millennial-scale changes to intensified NPIW  
59 and enhanced abyss flushing during deglacial cold and warm intervals, respectively,  
60 closely related to variations in North Atlantic Deep Water formation.

带格式的: 字体: 小四

带格式的: 字体: 小四

带格式的: 字体: 小四

带格式的: 字体: 小四

带格式的: 字体: 小四

带格式的: 字体: 小四

带格式的: 字体: (中文) +中文正文,  
小四

61        **Keywords:** sedimentary oxygenation; millennial timescale; North Pacific  
62    Intermediate Water; North Atlantic Deep Water; subtropical North Pacific



## 63 1. Introduction

64 A more sluggish deep ocean ventilation combined with a more efficient  
65 biological pump is widely thought to facilitate enhanced carbon sequestration in the  
66 ocean interior, leading to atmospheric CO<sub>2</sub> drawdown during glacial cold periods  
67 (Sigman and Boyle, 2000). These changes are tightly coupled to bottom water  
68 oxygenation and sedimentary redox changes on both millennial and orbital timescales  
69 (Hoogakker et al., 2015; Jaccard and Galbraith, 2012; Sigman and Boyle, 2000).  
70 Reconstruction of past sedimentary oxygenation is therefore crucial for understanding  
71 changes in export productivity and renewal of deep ocean circulation (Nameroff et al.,  
72 2004). Previous studies from North Pacific margins as well as open subarctic Pacific  
73 have identified drastic variations in export productivity and ocean oxygen levels at  
74 millennial and orbital timescales using diverse proxies such as trace elements  
75 (Cartapanis et al., 2011; Chang et al., 2014; Jaccard et al., 2009; Zou et al., 2012),  
76 benthic foraminiferal assemblages (Ohkushi et al., 2016; Ohkushi et al., 2013;  
77 Shibahara et al., 2007) and nitrogen isotopic composition ( $\delta^{15}\text{N}$ ) of organic matter  
78 (Addison et al., 2012; Chang et al., 2014; Galbraith et al., 2004; Riethdorf et al., 2016)  
79 in marine sediment cores. These studies suggested that both North Pacific  
80 Intermediate Water (NPIW) and export of organic matter regulate the sedimentary  
81 oxygenation variation during the last glaciation and Holocene in the subarctic Pacific.  
82 By contrast, little information exists on millennial-scale oxygenation changes to date  
83 in the western subtropical North Pacific (WSTNP).

84 The modern NPIW precursor waters are mainly sourced from the NW Pacific  
85 marginal seas (Shcherbina et al., 2003; Talley, 1993; You et al., 2000), spreading into  
86 the subtropical North Pacific at intermediate depths of 300 to 800 m (Talley, 1993).  
87 The pathway and circulation of NPIW have been identified by You (2003), who  
88 suggested that cabbeling, a mixing process to form a new water mass with increased  
89 density than that of parent water masses, is the principle mechanism responsible for  
90 transforming subpolar source waters into subtropical NPIW along the  
91 subarctic-tropical frontal zone. More specifically, a ~~lower-small~~ subpolar input of  
92 about 2 Sv (1 Sv = 10<sup>6</sup> m<sup>3</sup>/s) is sufficient for subtropical ventilation (You et al., 2003).

93 Benthic foraminiferal  $\delta^{13}\text{C}$ , a quasi-conservative tracer for water mass, from the North  
94 Pacific indicates an enhanced ventilation (higher  $\delta^{13}\text{C}$ ) at water depths of  $< 2000$  m  
95 during the last glacial period (Keigwin, 1998; Matsumoto et al., 2002). Furthermore,  
96 on the basis of both radiocarbon data and modeling results, Okazaki et al. (2010)  
97 suggested the formation of deep water in the North Pacific during the early  
98 deglaciation in Heinrich Stadial 1 (HS1). Enhanced NPIW penetration was further  
99 explored using numerical model simulations (Chikamoto et al., 2012; Gong et al.,  
100 2019; Okazaki et al., 2010). In contrast, substantial effects of intensified NPIW  
101 formation during Marine Isotope Stage (MIS) 2 and 6 on the ventilation and nutrient  
102 characteristics of lower latitude mid-depth Eastern Equatorial Pacific have been  
103 suggested by recent studies (Max et al., 2017; Rippert et al., 2017). The downstream  
104 effects of intensified NPIW are also reflected in the record of  $\delta^{13}\text{C}$  of *Cibicides*  
105 *wuellerstorfi* in core PN-3 from the middle Okinawa Trough (OT), where lower  
106 deglacial  $\delta^{13}\text{C}$  values were attributed to enhanced OC accumulation rates due to  
107 higher surface productivity by (Wahyudi and Minagawa, 1997).

108 The Okinawa Trough is separated from the Philippine Sea by the Ryukyu Islands  
109 and is an important channel of the northern extension of the Kuroshio in the WSTNP  
110 (Figure 1). Initially the OT opened at the middle Miocene (Sibuet et al., 1987) and  
111 since then, it has been a depositional center in the East China Sea (ECS), receiving  
112 large sediment supplies from nearby rivers (Chang et al., 2009). Surface  
113 oceanographic characteristics of the OT over glacial-interglacial cycles are largely  
114 influenced by the Kuroshio and ECS Coastal Water (Shi et al., 2014); the latter is  
115 related to the strength of summer East Asian monsoon (EAM) sourced from the  
116 western tropical Pacific. Modern physical oceanographic investigations showed that  
117 intermediate waters in the OT are mainly derived from horizontal advection and  
118 mixing of NPIW and South China Sea Intermediate Water (Nakamura et al., 2013).  
119 These waters intrude into the OT through two ways: (i) deeper part of the Kuroshio  
120 enters the OT through the channel east of Taiwan (sill depth 775 m) and (ii) through  
121 the Kerama Gap (sill depth 1100 m). In the northern OT, the subsurface water mainly  
122 flows through horizontal advection through the Kerama Gap from the Philippine Sea

123 (Nakamura et al., 2013). Recently, Nishina et al. (2016) found that an overflow  
124 through the Kerama Gap controls the modern deep-water ventilation in the southern  
125 OT.

126 Both surface characteristics and deep ventilation in the OT varied significantly  
127 since the last glaciation. During the last glacial period, the mainstream of the  
128 Kuroshio likely migrated to the east of the Ryukyu Islands or also became weaker due  
129 to lower sea levels (Shi et al., 2014; Ujiie and Ujiie, 1999; Ujiie et al., 2003) and the  
130 hypothetical emergence of a Ryukyu-Taiwan land bridge (Ujiie and Ujiie, 1999). In a  
131 recent study, based on the Mg/Ca-derived temperatures in surface and thermocline  
132 waters, and planktic foraminiferal indicators of water masses from two sediment cores  
133 located in the northern and southern OT, Ujiie et al. (2016) argued that the  
134 hydrological conditions of the North Pacific Subtropical Gyre since MIS 7 is  
135 modulated by the interaction between the Kuroshio and the NPIW. Besides the  
136 Kuroshio, the flux of East Asian rivers to the ECS, which is related to the summer  
137 EAM and the sea level oscillations coupled with topography have also been regulating  
138 the surface hydrography in the OT (Chang et al., 2009; Kubota et al., 2010; Sun et al.,  
139 2005; Yu et al., 2009).

140 Based on benthic foraminiferal assemblages, previous studies have implied a  
141 reduced oxygenation in deep waters of the middle and southern OT during the last  
142 deglacial period (Jian et al., 1996; Li et al., 2005), but a strong ventilation during the  
143 Last Glacial Maximum (LGM) and the Holocene (Jian et al., 1996; Kao et al., 2005).  
144 High sedimentary  $\delta^{15}\text{N}$  values, an indicator of increased denitrification in the  
145 subsurface water column, also occurred during the late deglaciation in the middle OT  
146 (Kao et al., 2008). Inconsistent with these results, Dou et al. (2015) suggested an oxic  
147 depositional environment during the last deglaciation in the southern OT based on  
148 weak positive cerium anomalies. Furthermore, Kao et al. (2006) hypothesized a  
149 reduced ventilation of deepwater in the OT during the LGM due to the reduction of  
150 KC inflow using a 3-D ocean model. Thus, the patterns and reasons that caused  
151 sedimentary oxygenation in the OT remain controversial.

## 152 **2. Paleo-redox proxies**

153 The sedimentary redox conditions are governed by the rate of oxygen supply from  
154 the overlying bottom water and the rate of oxygen removal from pore water (Jaccard  
155 et al., 2016), processes that are related to the supply of oxygen by ocean circulation  
156 and organic matter respiration, respectively. Contrasting geochemical behaviors of  
157 redox-sensitive trace metals (Mn, Mo, U, etc.) have been used to reconstruct bottom  
158 water and sedimentary oxygen changes (Algeo, 2004; Algeo and Lyons, 2006;  
159 Crusius et al., 1996; Dean et al., 1997; Tribovillard et al., 2006; Zou et al., 2012), as  
160 their concentrations readily respond to redox condition of the depositional  
161 environment (Morford and Emerson, 1999).

162 In general, enrichment of Mn with higher speciation states (Mn (III) and Mn (IV))  
163 in the form of Mn-oxide coatings is observed in marine sediments, when oxic  
164 conditions prevail into greater sediment depths as a result of low organic matter  
165 degradation rates and well-ventilated bottom water (Burdige, 1993). Under reducing  
166 conditions, the authigenic fraction of Mn (as opposed to its detrital background) is  
167 released as dissolved Mn (II) species into the pore water and thus its concentration is  
168 usually low in suboxic ( $O_2$  and  $HS^-$  absent) and anoxic ( $HS^-$  present) sediments. In  
169 addition, when Mn enrichment occurs in oxic sediments as solid phase Mn  
170 oxyhydroxides, it may lead to co-precipitation of other elements, such as Mo  
171 (Nameroff et al., 2002).

172 The elements Mo and U behave conservatively in oxygenated seawater, but are  
173 preferentially enriched in oxygen-depleted water (Morford and Emerson, 1999).  
174 However, these two trace metals behave differently in several ways. Molybdenum can  
175 be enriched in both oxic sediments, such as the near surface manganese-rich horizons  
176 in continental margin environments (Shimmield and Price, 1986) and in anoxic  
177 sediments (Nameroff et al., 2002). Under anoxic conditions, Mo can be reduced either  
178 from the +6 oxidation state to insoluble  $MoS_2$ , though this process is known to occur  
179 only under extremely reducing conditions, such as hydrothermal and/or diagenesis  
180 (Dahl et al., 2010; Helz et al., 1996) or be converted to particle-reactive  
181 thiomolybdates (Vorlicek and Helz, 2002). Zheng et al. (2000) suggested two critical  
182 thresholds for Mo scavenging from seawater: 0.1  $\mu M$  hydrogen sulfide ( $H_2S$ ) for

183 Fe-S-Mo co-precipitation and 100  $\mu\text{M}$   $\text{H}_2\text{S}$  for Mo scavenging as Mo-S or as  
184 particle-bound Mo without Fe. Although Crusius et al. (1996) noted insignificant  
185 enrichment of sedimentary Mo under suboxic conditions, Scott et al. (2008) argued  
186 that burial flux of Mo is not so low in suboxic environments. Excess concentration of  
187 Mo ( $\text{Mo}_{\text{excess}}$ ) in sediments thus suggests the accumulation of sediments either in  
188 anoxic ( $\text{H}_2\text{S}$  occurrence) or well oxygenated conditions (if  $\text{Mo}_{\text{excess}}$  is in association  
189 with Mn-oxides).

190 In general, U is enriched in anoxic sediments ( $>1 \mu\text{M}$   $\text{H}_2\text{S}$ ), but not in oxic  
191 sediments ( $>10 \mu\text{M}$   $\text{O}_2$ ) (Nameroff et al., 2002). Accumulation of U depends on the  
192 content of reactive organic matter (Sundby et al., 2004) and U precipitates as uraninite  
193 ( $\text{UO}_2$ ) during the conversion of Fe (III) to Fe (II) in suboxic conditions (Morford and  
194 Emerson, 1999; Zheng et al., 2002). One of the primary removal mechanisms for U  
195 from the ocean is via diffusion across the sediment-water interface of reducing  
196 sediments (Klinkhammer and Palmer, 1991). Under suboxic conditions, soluble U (VI)  
197 is reduced to insoluble U (IV), but free sulfide is not required for U precipitation  
198 (McManus et al., 2005). Jaccard et al. (2009) suggested that the presence of excess  
199 concentration of U ( $\text{U}_{\text{excess}}$ ) in the absence of Mo enrichment is indicative of a suboxic,  
200 but not sulfidic condition, within the diffusional range of the sediment-water interface.  
201 The felsic volcanism is also a primary source of uranium (Maithani and Srinivasan,  
202 2011). Therefore, the potential input of uranium from active volcanic sources around  
203 the northwestern Pacific to the adjacent sediments should not be neglected.

204 In this study, we investigate a suite of redox-sensitive elements and the ratio of  
205 Mo/Mn along with productivity proxies from a sediment core retrieved from the  
206 northern OT to reconstruct the sedimentary oxygenation in the WSTNP over the last  
207 50ka. Based on that, we propose that multiple factors, such as NPIW ventilation, the  
208 strength of the Kuroshio Current and export productivity, control the bottom  
209 sedimentary oxygenation in the OT on millennial timescales since the last glacial.

### 210 **3. Oceanographic setting**

211 Surface hydrographic characteristics of the OT are mainly controlled by the  
212 warmer, more saline, oligotrophic Kuroshio water and cooler, less saline, nutrient-rich

213 Changjiang Diluted Water, and the modern flow-path of the former is influenced by  
214 the bathymetry of the OT (Figure 1a). The Kuroshio Current originates from the  
215 North Equatorial Current and flows into the ECS from the Philippine Sea through the  
216 Suao-Yonaguni Depression. In the northern OT, Tsushima Warm Current (TWC), a  
217 branch of the Kuroshio, flows into the Japan Sea through the shallow Tsushima Strait.  
218 Volume transport of the Kuroshio varies seasonally due to the influence of the EAM  
219 with a maximum of 24 Sv in summer and a minimum of 20 Sv in autumn across the  
220 east of Taiwan (Qu and Lukas, 2003).

221 A lower sea surface salinity (SSS) zone in summer relative to the one in winter in  
222 the ECS migrates toward the east of OT, indicating enhanced impact of the  
223 Changjiang discharge associated with summer EAM (Figures 2a and 2b). An  
224 estimated ~80% of the mean annual discharge of the river Changjiang is supplied to  
225 the ECS (Ichikawa and Beardsley, 2002) and in situ observational data show a  
226 pronounced negative correlation between the Changjiang discharge and SSS in July  
227 (Delcroix and Murtugudde, 2002). Consistently, previous studies from the OT  
228 reported such close relationship between summer EAM and SSS back to the late  
229 Pleistocene (Chang et al., 2009; Clemens et al., 2018; Kubota et al., 2010; Sun et al.,  
230 2005).

231 Despite the effects of EAM and the Kuroshio, evidence of geochemical tracers  
232 (temperature, salinity, oxygen, nutrients and radiocarbon) collected during the World  
233 Ocean Circulation Experiment (WOCE) in the Pacific (transects P24 and P03) favors  
234 the presence of low salinity, nutrient-enriched intermediate and deep waters (Talley,  
235 2007). Dissolved oxygen content is  $<100 \mu\text{mol/kg}$  at water depths below 600 m in the  
236 OT, along WOCE transects PC03 and PC24 (Talley, 2007). Modern oceanographic  
237 observations at the Kerama Gap reveal that upwelling in the OT is associated with the  
238 inflow of NPIW and studies using a box model predicted that overflow through the  
239 Kerama Gap is responsible for upwelling ( $3.8\text{--}7.6 \times 10^{-6} \text{m s}^{-1}$ ) (Nakamura et al.,  
240 2013; Nishina et al., 2016).

## 241 **4. Materials and methods**

### 242 **4.1. Chronostratigraphy of core CSH1**

243 A 17.3 m long sediment core CSH1 (31° 13.7' N, 128° 43.4' E; water depth: 703  
244 m) was collected from the northern OT, close to the main stream of Tsushima Warm  
245 Current (TWC) (Figure 1b) and within the depth of NPIW (Figure 1c) using a piston  
246 corer during *Xiangyanghong09* Cruise in 1998, carried out by the First Institute of  
247 Oceanography, Ministry of Natural Resources of China. This location is enabling us  
248 to reconstruct millennial-scale changes in the properties of TWC and NPIW. Core  
249 CSH1 mainly consists of clayey silt and silt with occurrence of plant debris at some  
250 depth intervals (Ge et al., 2007) (Figure 3a). In addition, three layers of volcanic ash  
251 were observed at depths of 74–106 cm, 782–794 cm, 1570–1602 cm. These three  
252 intervals can be correlated with well-known ash layers, Kikai-Akahoya (K-Ah; 7.3  
253 ka), Aira-Tanzawa (AT; 29.24 ka) and Aso-4 (roughly around MIS 5a) (Machida,  
254 1999), respectively. The core was split and sub-sampled at 4 cm interval and then  
255 stored in the China Ocean Sample Repository at 4 °C until analysis.

256 Previously, paleoceanographic studies have been conducted and a set of data has  
257 been investigated for core CSH1, including the contents of planktic foraminifers as  
258 well as their carbon ( $\delta^{13}\text{C}$ ) and oxygen isotope ( $\delta^{18}\text{O}$ ) compositions (Shi et al., 2014),  
259 pollen (Chen et al., 2006), paleomagnetism (Ge et al., 2007) and  $\text{CaCO}_3$  (Wu et al.,  
260 2004). An age model for this core has been constructed by using ten Accelerator Mass  
261 Spectrometry (AMS)  $^{14}\text{C}$  dates and six oxygen isotope ( $\delta^{18}\text{O}$ ) age control points. The  
262 whole 17.3 m core contains *ca.* 88 ka-long record of continuous sedimentation (Shi et  
263 al., 2014).

264 Notably, the original age model, which used constant radiocarbon reservoir ages  
265 throughout core CSH1 are suitable to reveal orbital-scale Kuroshio variations (Shi et  
266 al., 2014), but insufficient to investigate millennial-scale climatic events. A higher  
267 abundance of *Neogloboquadrina pachyderma (dextral)*, e. g. that occurred during  
268 warmer intervals, such as the Bölling-Alleröd (B/A), has been challenging to explain.  
269 On the other hand, paired measurements of  $^{14}\text{C}/^{12}\text{C}$  and  $^{230}\text{Th}$  ages from Hulu Cave  
270 stalagmites suggest magnetic field changes have greatly contributed to high  
271 atmospheric  $^{14}\text{C}/^{12}\text{C}$  values at HS4 and the Younger Dryas (YD) (Cheng et al., 2018).  
272 Thus a constant reservoir age ( $\Delta R=0$ ) assumed when calibrating foraminiferal

273 radiocarbon dates using CALIB 6 software and the Marine 13 calibration dataset  
274 (Reimer et al., 2013) for core CSH1 may cause large chronological uncertainties.

275 Here, we recalibrated the radiocarbon dates using updated CALIB 7.04 software  
276 with Marine 13 calibration dataset (Reimer et al., 2013). Moreover, on the basis of  
277 significant correlation between planktic foraminifera species *Globigerinoides ruber*  
278  $\delta^{18}\text{O}$  and Chinese stalagmite  $\delta^{18}\text{O}$  (Cheng et al., 2016), a proxy of summer EAM  
279 related to SSS of the ECS, we improve the age model for core CSH1 (Figures 3b-3d).  
280 Overall, the new chronological framework is similar to the one previously reported by  
281 Shi et al. (2014), but with more dates. In order to compare with published results  
282 associated with ventilation changes in the North Pacific, here we mainly report the  
283 history of sedimentary oxygenation in the northern OT since the last glacial period.  
284 Linear sedimentation rate varied between ~10 and 40 cm/ka with higher  
285 sedimentation rates (around 30-40 cm/ka) between ~24 ka and 32.5 ka. Variation in  
286 sedimentation rate has been attributed to changes in eustatic sea level, summer EAM  
287 intensity, path and/or intensity of Kuroshio Current. Generally, sea level is thought to  
288 be the first-order factor for controlling linear sedimentation rate changes (Beny et al.,  
289 2018; Li et al., 2015; Zhao et al., 2017). The new age control points are shown in  
290 Table 2.

#### 291 4.2. Chemical analyses

292 Sediment subsamples for geochemical analyses were freeze-dried and ground to  
293 a fine powder with an agate mortar and pestle. Based on the age model, 85  
294 subsamples from core CSH1, representing a temporal resolution of about 600 years  
295 (every 4 cm interval) were selected for detailed geochemical analyses of major and  
296 minor elements, and total carbon (TC), organic carbon (TOC) and nitrogen (TN)  
297 contents. The pretreatment of sediment and other analytical methods have been  
298 reported elsewhere (Zou et al., 2012).

299 TC and TN were determined with an elemental analyzer (EA; Vario EL III,  
300 Elementar Analysen systeme GmbH) in the Key Laboratory of Marine Sediment and  
301 Environment Geology, First Institute of Oceanography, Ministry of Natural Resources  
302 of China, Qingdao. Carbonate was removed from sediments by adding 1M HCl to the

带格式的: 字体颜色: 自动设置

带格式的: 字体颜色: 自动设置

带格式的: 字体颜色: 自动设置

带格式的: 字体: (中文) 楷体, 字体颜色: 自定义颜色 (RGB (0, 0, 204))



303 homogenized sediments for total organic carbon (TOC) analysis using the same  
304 equipment. The content of calcium carbonate (CaCO<sub>3</sub>) was calculated using the  
305 equation:

$$306 \quad \text{CaCO}_3 = (\text{TC} - \text{TOC}) \times 8.33$$

307 where 8.33 is the ratio between the molecular weight of carbonate and the atomic  
308 weight of carbon. National reference material (GSD-9), blank sample and replicated  
309 samples were used to control the analytical process. The relative standard deviation of  
310 the GSD-9 for TC, TN and TOC is  $\leq 3.4\%$ .

311 About 0.5 g of sediment powder was digested in double distilled HF:HNO<sub>3</sub> (3:1),  
312 followed by concentrated HClO<sub>4</sub>, and then re-dissolved in 5% HNO<sub>3</sub>. Selected major  
313 and minor elements such as aluminum (Al) and manganese (Mn) were determined by  
314 inductively coupled plasma optical emission spectroscopy (ICP-OES; Thermo  
315 Scientific iCAP 6000, Thermo Fisher Scientific), as detailed elsewhere (Zou et al.,  
316 2012). In addition, Mo and U were analyzed with inductively coupled plasma mass  
317 spectrometry (ICP-MS; Thermo Scientific XSERIES 2, Thermo Fisher Scientific), as  
318 described in Zou et al. (2012). Precision for most elements in the reference material  
319 GSD-9 is  $\leq 5\%$  relative standard deviation. The excess fractions of U and Mo were  
320 estimated by normalization to Al:

$$321 \quad \text{Excess fraction} = \frac{\text{total}_{\text{element}} - (\text{element}/\text{Al}_{\text{average shale}} \times \text{Al})}{\text{Al}_{\text{average shale}}}, \text{ with } \text{U}/\text{Al}_{\text{average shale}} =$$
$$322 \quad 0.307 \times 10^{-6} \text{ and } \text{Mo}/\text{Al}_{\text{average shale}} = 0.295 \times 10^{-6} \text{ (Li and Schoonmaker, 2014).}$$

323 In addition, given the different geochemical behaviors of Mn and Mo and  
324 co-precipitation and adsorption processes associated with the redox cycling of Mn, we  
325 calculated the ratio of Mo to Mn, assuming that higher Mo/Mn ratio indicates lower  
326 oxygen content in the depositional environment and vice versa. In combination with  
327 the concentration of excess uranium, we infer the history of sedimentary oxygenation  
328 in the subtropical North Pacific since the last glaciation.

## 329 **5. Results**

### 330 **5.1. TOC, TN, and CaCO<sub>3</sub>**

331 The content of CaCO<sub>3</sub> varies from 8.8 to 35% (Figure 4a) and it mostly shows  
332 higher values with increasing trends during the last deglaciation. In contrast, the

333 content of CaCO<sub>3</sub> is low and exhibits decreasing trends during the late MIS 3 and the  
334 LGM (Figure 4a). TN content shows a larger variation compared to TOC (Figure 4b),  
335 but it still strongly correlates with TOC ( $r = 0.74$ ,  $p < 0.01$ ) throughout the entire core.  
336 Concentration of TOC ranges from 0.5 to 2.1% and it shows higher values with stable  
337 trends during the last glacial phase (MIS 3) (Figure 4c). Molar ratios of TOC/TN vary  
338 around 10, with higher ratios at the transition into the LGM (Figure 4d),  
339 corresponding to higher linear sedimentation rate (Figure 4e).

340 Both TOC and CaCO<sub>3</sub> have been used as proxies for the reconstruction of past  
341 export productivity (Cartapanis et al., 2011; Lembke-Jene et al., 2017; Rühlemann et  
342 al., 1999). Molar C/N ratios of  $>10$  (Figure 4c) suggest that terrigenous organic  
343 sources significantly contribute to the TOC concentration in core CSH1. The TOC  
344 content therefore may be not a reliable proxy for the reconstruction of surface water  
345 export productivity during times of the LGM and late deglaciation, when maxima in  
346 C/N ratios co-occur with decoupled trends between CaCO<sub>3</sub> and TOC concentrations.

347 Several lines of evidence support CaCO<sub>3</sub> as a reliable productivity proxy,  
348 particularly during the last deglaciation. The strong negative correlation coefficient ( $r$   
349  $= -0.85$ ,  $p < 0.01$ ) between Al and CaCO<sub>3</sub> in sediments throughout core CSH1  
350 confirms the biogenic origin of CaCO<sub>3</sub> against terrigenous Al (Figure 4f). Generally,  
351 terrigenous dilution decreases the concentrations of CaCO<sub>3</sub>. An inconsistent  
352 relationship between CaCO<sub>3</sub> contents and sedimentation rates indicates a minor effect  
353 of dilution on CaCO<sub>3</sub>. Furthermore, the increasing trend in CaCO<sub>3</sub> associated with  
354 high sedimentation rate during the last deglacial interval indicates a substantial  
355 increase in export productivity (Figures 4a and 4d). The high coherence between  
356 CaCO<sub>3</sub> content and alkenone-derived sea surface water (SST) (Shi et al., 2014)  
357 indicates a direct control on CaCO<sub>3</sub> by SST. Moreover, a detailed comparison between  
358 CaCO<sub>3</sub> concentrations and the previously published foraminiferal fragmentation ratio  
359 (Wu et al., 2004) shows, apart from a small portion within the LGM, no clear  
360 co-variation between them. These pieces of evidence suggest that CaCO<sub>3</sub> changes are  
361 driven primarily by variations in carbonate primary production, and not overprinted  
362 by secondary processes, such as carbonate dissolution through changes in the

363 lysocline depth and dilution by terrigenous materials. Likewise, a similar deglacial  
364 trend in  $\text{CaCO}_3$  is also observed in core MD01-2404 (Chang et al., 2009), indicating a  
365 ubiquitous, not local picture in the OT. All these lines of evidence thus support  $\text{CaCO}_3$   
366 of core CSH1 as a reliable productivity proxy to a first order approximation.

## 367 **5.2. Redox-sensitive Elements**

368 Figure 4 shows time series of selected redox-sensitive elements (RSEs) and  
369 proxies derived from them. Mn shows higher concentrations during the LGM and  
370 HS1 (16 ka–22 ka) and middle-late Holocene, but lower concentrations during the last  
371 deglacial and Preboreal periods (15.8 ka–9.5 ka, Figure 4g). Generally, concentrations  
372 of excess Mo and excess U (Figures 4j and 4l) show coherent patterns with those of  
373 Mo and U (Figures 4i and 4k), but both are out-of-phase with Mn over the last glacial  
374 period (Figure 4h). Pronounced variations in U concentration after 8.5 ka are related  
375 to the occurrence of discrete volcanic materials. A significant positive Eu anomaly  
376 (Zhu et al., 2015) confirms the occurrence of discrete volcanic materials and its  
377 dilution effects on terrigenous components since 7 ka. Occurrence of discrete volcanic  
378 material is likely related to intensified Kuroshio Current during the mid-late Holocene,  
379 as supported by higher hydrothermal Hg concentrations in sediments from the middle  
380 OT (Lim et al., 2017). A negative correlation between Mn and  $\text{Mo}_{\text{excess}}$  during the last  
381 glaciation and the Holocene, and the strong positive correlation between them during  
382 the LGM and HS1 (Figures 5a and 5b) further corroborate the complex geochemical  
383 behaviors of Mn and Mo. A strong positive correlation between  $\text{Mo}_{\text{excess}}$  and Mn  
384 (Figure 5b) may be attributed to co-precipitation of Mo by Mn-oxyhydroxide under  
385 oxygenated conditions. Here, we thus use the Mo/Mn ratio, instead of excess Mo  
386 concentration to reconstruct variations in sedimentary redox conditions in our study  
387 area. Overall, the Mo/Mn ratio shows similar downcore pattern to that of  $\text{Mo}_{\text{excess}}$  with  
388 higher ratios during the last deglaciation, but lower ratios during the LGM and HS1. A  
389 strong correlation ( $r = 0.69$ ) between Mo/Mn ratio and excess U concentration  
390 (excluding the data of Holocene, due to the contamination with volcanic material,  
391 Figure 5c) further corroborates the integrity of Mo/Mn as an indicator of sedimentary  
392 oxygenation changes.

393 Rapidly decreasing Mo/Mn ratios indicate a well oxygenated sedimentary  
394 environment after ~8 ka (Figure 4h). Both higher Mo/Mn ratios and excess U  
395 concentrations, together with lower Mn concentrations suggest suboxic depositional  
396 conditions during the late deglacial period (15.8 ka–9.5 ka), whereas lower ratios  
397 during the LGM, HS1 and HS2 indicate relatively better oxygenated sedimentary  
398 conditions. A decreasing trend in Mo/Mn ratio and excess U concentration from 50 ka  
399 to 25 ka also suggest higher sedimentary oxygen levels.

## 400 **6. Discussion**

### 401 **6.1. Constraining paleoredox conditions in the Okinawa Trough**

402 In general, three different terms, hypoxia, suboxia and anoxia, are widely used to  
403 describe the degree of oxygen depletion in the marine environment (Hofmann et al.,  
404 2011). Here, we adopt the definition of oxygen thresholds by Bianchi et al. (2012) for  
405 oxic ( $>120 \mu\text{mol/kg O}_2$ ), hypoxic ( $<60\text{--}120 \mu\text{mol/kg O}_2$ ) and suboxic ( $<2\text{--}10$   
406  $\mu\text{mol/kg O}_2$ ) conditions, whereas anoxia is the absence of measurable oxygen.

407 Proxies associated with RSEs, such as sedimentary Mo concentration (Lyons et  
408 al., 2009; Scott et al., 2008) have been used to constrain the degree of oxygenation in  
409 seawater. Algeo and Tribovillard (2009) proposed that open-ocean systems with  
410 suboxic waters tend to yield  $U_{\text{excess}}$  enrichment relative to  $Mo_{\text{excess}}$ , resulting in  
411 sediment  $(Mo/U)_{\text{excess}}$  ratio less than that of seawater (7.5-7.9). Under increasingly  
412 reducing and occasionally sulfidic conditions, the accumulation of  $Mo_{\text{excess}}$  increase  
413 relative to that of  $U_{\text{excess}}$  leading the  $(Mo/U)_{\text{excess}}$  ratio either is equal to or exceeds  
414 with that of seawater. Furthermore, Scott and Lyons (2012) suggested a non-euxinic  
415 condition with the presence of sulfide in pore waters, when Mo concentrations range  
416 from  $> 2 \mu\text{g/g}$ , the crustal average to  $< 25 \mu\text{g/g}$ , a threshold concentration for euxinic  
417 condition. Given that the northern OT is located in an open oceanic setting, we use  
418 these two proxies to evaluate the degree of oxygenation in sediments.

419 Both bulk Mo concentration (1.2-9.5  $\mu\text{g/g}$ ) and excess (Mo/U) ratio (0.2-5.7) in  
420 core CSH1 suggest that oxygen-depleted conditions have prevailed in the deep water  
421 of the northern OT over the last 50 ka (Figure 4m). However, increased excess Mo  
422 concentrations with higher Mo/U ratios during the last termination (18 ka-9 ka)

423 indicate more reducing conditions compared to the Holocene and the last glacial  
424 period, though Mo concentrations were less than 25  $\mu\text{g/g}$ , a threshold for euxinic  
425 deposition proposed by Scott and Lyons (2012).

426 The relative abundance of benthic foraminifera species that thrive in different  
427 oxygen concentrations has also been widely used to reconstruct variations in bottom  
428 water ventilation, such as the enhanced abundance of *Bulimina aculeata*, *Uvigerina*  
429 *peregrina* and *Chilostomella oolina* found under oxygen-depleted conditions in the  
430 central and southern OT from 18 ka to 9.2 ka (Jian et al., 1996; Li et al., 2005). An  
431 oxygenated bottom water condition is also indicated by abundant benthic foraminifera  
432 species *Cibicoides hyalina* and *Globocassidulina subglobosa* after 9.2 ka (Jian et al.,  
433 1996; Li et al., 2005) in cores E017 (1826 m water depth) and 255 (1575 m water  
434 depth) and high benthic  $\delta^{13}\text{C}$  values (Wahyudi and Minagawa, 1997) in core PN-3  
435 (1058 m water depth) from the middle and southern OT during the postglacial period.  
436 The poorly-ventilated deep water in the middle and southern OT inferred by benthic  
437 foraminiferal assemblages during the last deglaciation correlates with the one in the  
438 northern OT referring to our RSEs (Figure 4). A link thus can be hypothesized  
439 between deep-water ventilation and sedimentary oxygenation in the OT. Overall, a  
440 combination of our proxy records of RSEs in core CSH1 with other records shows  
441 oxygen-rich conditions during the last glaciation and middle and late Holocene (since  
442 8.5 ka) intervals, but oxygen-poor conditions during the last deglaciation.

## 443 **6.2. Causes for sedimentary oxygenation variations**

444 Our observed pattern of RSEs in core CSH1 suggests that drastic changes in  
445 sedimentary oxygenation occurred on orbital and millennial timescales over the last  
446 glaciation in the OT. In general, four factors can regulate the redox condition in the  
447 deep water column: (i)  $\text{O}_2$  solubility, (ii) export productivity and subsequent  
448 degradation of organic matter, (iii) vertical mixing, and (iv) lateral supply of oxygen  
449 through intermediate and deeper water masses (Ivanochko and Pedersen, 2004;  
450 Jaccard and Galbraith, 2012). These processes have been invoked in previous studies  
451 to explain the deglacial Pacific-wide variations in oxygenation by either one or a  
452 combination of these factors (Galbraith and Jaccard, 2015; Moffitt et al., 2015;

453 Praetorius et al., 2015). Our data also suggest drastic variations in sedimentary  
454 oxygenation over the last 50 ka. However, the mechanisms responsible for  
455 sedimentary oxygenation variations in the basin-wide OT and its connection with  
456 ventilation of the open North Pacific remain unclear. In order to place our core results  
457 in a wider regional context, we compare our proxy records of sedimentary  
458 oxygenation ( $U_{\text{excess}}$  concentration and Mo/Mn ratio) and export productivity ( $\text{CaCO}_3$ )  
459 (Figures 6a, ~~b~~, ~~c~~) with abundance of *Pulleniatina obliquiloculata* (an indicator of  
460 Kuroshio strength) and sea surface temperature (Shi et al., 2014), bulk sedimentary  
461 nitrogen isotope (an indicator of denitrification) (Kao et al., 2008), benthic  
462 foraminifera  $\delta^{13}\text{C}$  (a proxy for ventilation) in cores PN-3 and PC23A (Rella et al.,  
463 2012; Wahyudi and Minagawa, 1997), abundance of benthic foraminifera (an  
464 indicator of hypoxia) in core E017 (Li et al., 2005) and ODP Site 1017 (Cannariato  
465 and Kennett, 1999) (Figures 6d-~~e~~k).

#### 466 **6.2.1. Effects of regional ocean temperature on deglacial deoxygenation**

467 Warming ocean temperatures lead to lower oxygen solubility. In the geological  
468 past, solubility effects connected to temperature changes of the water column thought  
469 to enhance or even trigger hypoxia (Praetorius et al., 2015). Shi et al. (2014) reported  
470 an increase in SST of around  $4^\circ\text{C}$  (from  $\sim 21^\circ\text{C}$  to  $\sim 24.6^\circ\text{C}$ ) during the last  
471 deglaciation in core CSH1 (Figure 6d). Based on thermal solubility effects, a  
472 hypothetical warming of  $1^\circ\text{C}$  would reduce oxygen concentrations by about 3.5  
473  $\mu\text{mol/kg}$  at water temperatures around  $22^\circ\text{C}$  (Brewer and Peltzer, 2016), therefore a  $\sim$   
474  $4^\circ\text{C}$  warming at core CSH1 (Shi et al., 2014) could drive a conservative estimate of a  
475 drop of  $<15 \mu\text{mol/kg}$  in oxygen concentration, assuming no large salinity changes.  
476 However, given the semi-quantitative nature of our data about oxygenation changes,  
477 which seemingly exceed an amplitude of  $>15 \mu\text{mol/kg}$ , we suggest that other factors,  
478 e.g. local changes in export productivity, regional influences such as vertical mixing  
479 due to changes of the Kuroshio Current, and far-field effects may have played  
480 decisive roles in shaping the oxygenation history of the OT.

#### 481 **6.2.2. Links between deglacial primary productivity and sedimentary** 482 **deoxygenation**

483 Previous studies have suggested the occurrence of high primary productivity in  
484 the entire OT during the last deglacial period (Chang et al., 2009; Jian et al., 1996;  
485 Kao et al., 2008; Li et al., 2017; Shao et al., 2016; Wahyudi and Minagawa, 1997).  
486 Such an increase in export production was due to favorable conditions for  
487 phytoplankton blooms, which were likely induced by warm temperatures and maxima  
488 in nutrient availability, the latter being mainly sourced from increased discharge of  
489 the Changjiang River, erosion of material from the ongoing flooding of the shallow  
490 continental shelf in the ECS, and upwelling of Kuroshio Intermediate Water (Chang  
491 et al., 2009; Li et al., 2017; Shao et al., 2016; Wahyudi and Minagawa, 1997). On the  
492 basis of sedimentary reactive phosphorus concentration, Li et al. (2017) concluded  
493 that export productivity increased during warm episodes but decreased during cold  
494 spells on millennial timescales over the last 91 ka in the OT. Gradually increasing  
495 concentrations of CaCO<sub>3</sub> in core CSH1 during the deglaciation (Figure 6a) and little  
496 changes in foraminiferal fragmentation ratios (Wu et al., 2004), are indicative of high  
497 export productivity in the northern OT. Accordingly, our data indicate that an increase  
498 in export productivity during the last deglaciation, which was previously evidenced by  
499 concentrations of reactive phosphorus (Li et al., 2017) and CaCO<sub>3</sub> (Chang et al., 2009)  
500 from the middle OT, and thus was a pervasive, synchronous phenomenon in the entire  
501 study region at the outermost extension of the ECS.

502 Similar events of high export productivity have been reported in the entire North  
503 Pacific due to increased nutrient supply, high SST, reduced sea ice cover, etc.  
504 (Crusius et al., 2004; Dean et al., 1997; Galbraith et al., 2007; Jaccard and Galbraith,  
505 2012; Kohfeld and Chase, 2011). In most of these cases, increased export productivity  
506 were-was thought to be responsible for oxygen depletion in mid-depth waters, due to  
507 exceptionally high oxygen consumption. However, the productivity changes during  
508 the deglacial interval, very specifically CaCO<sub>3</sub>, are not fully consistent with the trends  
509 of excess U and Mo/Mn ratio (Figures 6b and 6c). The sedimentary oxygenation thus  
510 cannot be determined by export productivity alone.

### 511 **6.2.3 Effects of the Kuroshio dynamics on sedimentary oxygenation**

512 The Kuroshio Current, one of the main drivers of vertical mixing, has been

513 identified as the key factor in controlling modern deep ventilation in the OT (Kao et  
514 al., 2006). However, the flow path of the Kuroshio in the OT during the glacial  
515 interval remains a matter of debate. Planktic foraminiferal assemblages in sediment  
516 cores from inside and outside the OT indicated that the Kuroshio migrated to the east  
517 of the Ryukyu Islands during the LGM (Ujiié and Ujiié, 1999). Subsequently, Kao et  
518 al. (2006) based on modeling results suggested that the Kuroshio still enters the OT,  
519 but the volume transport was reduced by 43% compared to the present-day transport  
520 and the outlet of Kuroshio switches from the Tokara Strait to the Kerama Gap at -80  
521 and -135m lowered sea level. Combined with sea surface temperature (SST) records  
522 and ocean model results, Lee et al. (2013) argued that there was little effect of  
523 deglacial sea-level change on the path of the Kuroshio, which still exited the OT from  
524 the Tokara Strait during the glacial period. Because the main stream of the Kuroshio  
525 Current is at a water depth of ~150 m, the SST records are insufficient to decipher past  
526 changes of the Kuroshio (Ujiié et al., 2016). On the other hand, low abundances of *P.*  
527 *obliquiloculata* in core CSH1 in the northern OT (Figure 6e) indicate that the main  
528 flow path of the Kuroshio migrated to the east of the Ryukyu Island (Shi et al., 2014).  
529 Such a flow change would have been caused by the proposed block of the  
530 Ryukyu-Taiwan land bridge by low sea level (Ujiié and Ujiié, 1999) and an overall  
531 reduced Kuroshio intensity (Kao et al., 2006), effectively suppressing the effect of the  
532 Kuroshio on deep ventilation in the OT. Our RSEs data show that oxygenated  
533 sedimentary conditions were dominant in the northern OT throughout the last glacial  
534 period (Figures 6b and 6c). The Kuroshio thus likely had a weak or even no effect on  
535 the renewal of oxygen to the sedimentary environment during the last glacial period.  
536 More recently, lower hydrothermal total Hg concentration during 20 ka - 9.6 ka,  
537 associated with reduced intensity and/or variation in flow path of KC, relative to that  
538 of Holocene recorded in core KX12 - 3 (1423 water depth) (Lim et al., 2017), further  
539 validates our inference.

540 On the other hand, the gradually increased alkenone-derived SST and abundance  
541 of *P.obliquiloculata* (Figures 6d and 6e) from 15 ka onwards indicates an intensified  
542 Kuroshio Current. At present, mooring and float observations revealed that the KC



543 penetrates to 1200 m isobath in the East China Sea (Andres et al., 2015). However,  
544 the effect of Kuroshio on sedimentary oxygenation was likely very limited during the  
545 glacial period and only gradually increasing throughout the last glacial termination.  
546 Therefore, while its effect on our observed deglacial variation in oxygenation may  
547 provide a slowly changing background condition in vertical mixing effects on the  
548 sedimentary oxygenation in the OT, it cannot account for the first order, rapid  
549 oxygenation changes, including indications for millennial-scale variations, that we  
550 observe between 18 ka and 9 ka.

551 Better oxygenated sedimentary conditions since 8.5 ka coincided with intensified  
552 Kuroshio (Li et al., 2005; Shi et al., 2014), as indicated by rapidly increased SST and  
553 *P. obliquiloculata* abundance in core CSH1 (Figures 6d and 6e) and *C. hyaline*  
554 abundance in core E017 (Figure 6i). Re-entrance of the Kuroshio into the OT (Shi et  
555 al., 2014) with rising eustatic sea level likely enhanced the vertical mixing and  
556 exchange between bottom and surface waters, ventilating the deep water in the OT.  
557 Previous comparative studies based on epibenthic  $\delta^{13}\text{C}$  values indicated  
558 well-ventilated deep water feeding both inside the OT and outside off the Ryukyu  
559 Islands during the Holocene (Kubota et al., 2015; Wahyudi and Minagawa, 1997). In  
560 summary, enhanced sedimentary oxygenation regime observed in the OT during the  
561 Holocene is mainly related to the intensified Kuroshio, while the effect of the  
562 Kuroshio on OT oxygenation was limited before 15 ka.

#### 563 **6.2.4. Effects of GNPIW on sedimentary oxygenation**

564 Relatively stronger oxygenated Glacial North Pacific Intermediate Water  
565 (GNPIW), coined by (Matsumoto et al., 2002), has been widely documented in the  
566 Bering Sea (Itaki et al., 2012; Kim et al., 2011; Rella et al., 2012), the Okhotsk Sea  
567 (Itaki et al., 2008; Okazaki et al., 2014; Okazaki et al., 2006; Wu et al., 2014), off east  
568 Japan (Shibahara et al., 2007), the eastern North Pacific (Cartapanis et al., 2011;  
569 Ohkushi et al., 2013) and western subarctic Pacific (Keigwin, 1998; Matsumoto et al.,  
570 2002). The intensified formation of GNPIW due to additional source region in the  
571 Bering Sea was proposed by Ohkushi et al. (2003) and Horikawa et al. (2010). Under  
572 such conditions, the invasion of well-ventilated GNPIW into the OT through the

573 Kerama Gap would have replenished the water column oxygen in the OT, although  
574 the penetration depth of GNPIW remains under debate (Jaccard and Galbraith, 2013;  
575 Max et al., 2014; Okazaki et al., 2010; Rae et al., 2014). Both a gradual decrease in  
576 excess U concentration and an increase in Mo/Mn ratio during the last glacial period  
577 (25 ka-50 ka) validate such inference, suggesting pronounced effects of intensified  
578 NPIW formation in the OT.

579 During HS1, a stronger formation of GNPIW was supported by proxy studies  
580 and numerical simulations. For example, on the basis of paired benthic-planktic (B-P)  
581 <sup>14</sup>C data, enhanced penetration of NPIW into a much deeper water depth during HS1  
582 relative to the Holocene has been revealed in several studies (Max et al., 2014;  
583 Okazaki et al., 2010; Sagawa and Ikehara, 2008), which was also simulated by several  
584 models (Chikamoto et al., 2012; Gong et al., 2019; Okazaki et al., 2010). On the other  
585 hand, increased intermediate water temperature in the subtropical Pacific recorded in  
586 core GH08-2004 (1166 m water depth) (Kubota et al., 2015) and young deep water  
587 observed in the northern South China Sea during HS1 (Wan and Jian, 2014) along  
588 downstream region of NPIW are also related to intensified NPIW formation.  
589 Furthermore, the pathway of GNPIW from numerical model simulations (Zheng et al.,  
590 2016) was similar to modern observations (You, 2003). Thus, all these evidence imply  
591 a persistent, cause and effect relation between GNPIW ventilation, the intermediate  
592 and deep water oxygen concentration in the OT and sediment redox state during HS1.  
593 In addition, our RSEs data also suggested a similarly enhanced ventilation in HS2  
594 (Figures 6b and 6c) that is also attributed to intensified GNPIW formation.

595 Hypoxic conditions during the B/A have been also widely observed in the mid-  
596 and high-latitude North Pacific (Jaccard and Galbraith, 2012; Praetorius et al., 2015).  
597 Our data of excess U concentration and Mo/Mn ratio recorded in core CSH1 (Figures  
598 6b and 6c), together with enhanced denitrification and *B. aculeata* abundance (Figures  
599 6f and 6h), further reveal the expansion of oxygen-depletion at mid-depth waters  
600 down to the subtropical NW Pacific during the late deglacial period. Based on high  
601 relative abundances of radiolarian species, indicators of upper intermediate water  
602 ventilation in core PC-23A, Itaki et al. (2012) suggested that a presence of

603 well-ventilated waters was limited to the upper intermediate layer (200 m–500 m) in  
604 the Bering Sea during warm periods, such as the B/A and Preboreal. Higher B-P  
605 foraminiferal  $^{14}\text{C}$  ages, together with increased temperature and salinity at  
606 intermediate waters recorded in core GH02-1030 (off East Japan) supported a  
607 weakened formation of NPIW during the B/A (Sagawa and Ikehara, 2008). These  
608 lines of evidence indicate that the boundary between GNPIW and North Pacific Deep  
609 Water shoaled during the B/A, in comparison to HS1. Based on a comparison of two  
610 benthic foraminiferal oxygen and carbon isotope records from off northern Japan and  
611 the southern Ryukyu Island, Kubota et al. (2015) found a stronger influence of Pacific  
612 Deep Water on intermediate-water temperature and ventilation at their southern than  
613 the northern locations, though both sites are located at similar water depths (1166 m  
614 and 1212 m for cores GH08-2004 and GH02-1030, respectively). Higher excess U  
615 concentration and low Mo/Mn ratio in our core CSH1 during the B/A and Preboreal  
616 suggest reduced sedimentary oxygenation, consistent with reduced ventilation of  
617 GNPIW, contributing to the subsurface water deoxygenation in the OT.

618 During the YD, both Mo/Mn ratio and excess U show a slightly decreased  
619 oxygen condition in the northern OT. By contrast, benthic foraminiferal  $\delta^{18}\text{O}$  and  $\delta^{13}\text{C}$   
620 values in a sediment core collected from the Oyashio region suggested a strengthened  
621 formation and ventilation of GNPIW during the YD (Ohkushi et al., 2016). This  
622 pattern possibly indicates a time-dependent, varying contribution of distal GNPIW to  
623 the deglacial OT oxygenation history, and we presume a more pronounced  
624 contribution of organic matter degradation due to high export productivity during this  
625 period, as suggested by increasing  $\text{CaCO}_3$  content.

### 626 **6.3. Subtropical North Pacific ventilation links to North Atlantic Climate**

627 One of the characteristic climate features in the Northern Hemisphere, in  
628 particular the North Atlantic is millennial-scale oscillation during glacial and deglacial  
629 periods. These abrupt climatic events have been widely thought to be closely related  
630 to varying strength of Atlantic Meridional Overturning Circulation (AMOC)  
631 (Lynch-Stieglitz, 2017). One of dynamic proxies of ocean circulation,  $^{231}\text{Pa}/^{230}\text{Th}$   
632 reveals that severe weakening of AMOC only existed during Heinrich stadials due to

633 increased freshwater discharges into the North Atlantic (Böhm et al., 2015; McManus  
634 et al., 2004). On the other hand, several mechanisms, such as sudden termination of  
635 freshwater input (Liu et al., 2009), atmospheric CO<sub>2</sub> concentration (Zhang et al.,  
636 2017), enhanced advection of salt (Barker et al., 2010) and changes in background  
637 climate (Knorr and Lohmann, 2007) were proposed to explain the reinvigoration of  
638 AMOC during the B/A.

639 Our RSEs data in the Northern OT and endobenthic  $\delta^{13}\text{C}$  in the Bering Sea  
640 (Figures 7a-7c) both show a substantial millennial variability in intermediate water  
641 ventilation in the subtropical North Pacific. Notably, enhanced ventilation during HS1  
642 and HS2 and oxygen-poor condition during the B/A respectively correspond to the  
643 collapse and resumption of AMOC (Figure 7d). Such out-of-phase millennial-scale  
644 pattern is consistent with the results of various modeling simulations (Chikamoto et  
645 al., 2012; Menviel et al., 2014; Okazaki et al., 2010; Saenko et al., 2004), although  
646 these models had different boundary conditions and causes for the observed effects in  
647 GNPIW formation, and ventilation ages derived from B-P  $^{14}\text{C}$  (Freeman et al., 2015;  
648 Max et al., 2014; Okazaki et al., 2012). These lines of evidence confirm a persistent  
649 link between the ventilation of North Pacific and the North Atlantic climate  
650 (Lohmann et al., 2019). Such links have also been corroborated by proxy data and  
651 modeling experiment between AMOC and East Asian monsoon during the 8.2 ka  
652 event (Liu et al., 2013), the Holocene (Wang et al., 2005) and 34 ka–60 ka (Sun et al.,  
653 2012). The mechanism linking East Asia with North Atlantic has been attributed to an  
654 atmospheric teleconnection, such as the position and strength of Westerly Jet and  
655 Mongolia-Siberian High (Porter and Zhisheng, 1995). However, the mechanism  
656 behind such out-of-phase pattern between the ventilation in the subtropical North  
657 Pacific and the North Atlantic deep water formation remains unclear.

658 Increased NPIW formation during HS1 may have been caused by enhanced  
659 salinity-driven vertical mixing through higher meridional water mass transport from  
660 the subtropical Pacific. Previous studies have proposed that intermediate water  
661 formation in the North Pacific hinged on a basin-wide increase in sea surface salinity  
662 driven by changes in strength of the summer EAM and the moisture transport from

663 the Atlantic to the Pacific (Emile-Geay et al., 2003). Several modeling studies found  
664 that freshwater forcing in the North Atlantic could cause a widespread surface  
665 salinification in the subtropical Pacific Ocean (Menviel et al., 2014; Okazaki et al.,  
666 2010; Saenko et al., 2004). This idea has been tested by proxy data (Rodríguez-Sanz  
667 et al., 2013; Sagawa and Ikehara, 2008), which indicated a weakened summer EAM  
668 and reduced transport of moisture from Atlantic to Pacific through Panama Isthmus  
669 owing to the southward displacement of Intertropical Convergence Zone caused by a  
670 weakening of AMOC. Along with this process, as predicted through a general  
671 circulation modeling, a strengthened Pacific Meridional Overturning Circulation  
672 would have transported more warm and salty subtropical water into the high-latitude  
673 North Pacific (Okazaki et al., 2010). In accordance with comprehensive Mg/Ca  
674 ratio-based salinity reconstructions, however, Riethdorf et al. (2013) found no clear  
675 evidence for such higher salinity patterns in the subarctic northwest Pacific during  
676 HS1.

677 On the other hand, a weakened AMOC would deepen the wintertime Aleutian  
678 Low based on modern observation (Okumura et al., 2009), which is closely related to  
679 the sea ice formation in the marginal seas of the subarctic Pacific (Cavalieri and  
680 Parkinson, 1987). Once stronger Aleutian Low, intense brine rejection due to sea ice  
681 expansion, would have enhanced the NPIW formation. Recently modeling-derived  
682 evidence confirmed that enhanced sea ice coverage occurred in the southern Okhotsk  
683 Sea and off East Kamchatka Peninsula during HS1 (Gong et al., 2019). In addition,  
684 stronger advection of low-salinity water via the Alaskan Stream to the subarctic NW  
685 Pacific was probably enhanced during HS1, related to a shift of the Aleutian Low  
686 pressure system over the North Pacific, which could also increase sea ice formation,  
687 brine rejection and thereafter intermediate water ventilation (Riethdorf et al., 2013).

688 During the late deglaciation, ameliorating global climate conditions, such as  
689 warming Northern Hemisphere, and a strengthened Asian summer monsoon, are a  
690 result of changes in insolation forcing, greenhouse gases concentrations, and variable  
691 strengths of the AMOC (Clark et al., 2012; Liu et al., 2009). During the B/A, a  
692 decrease in sea ice extent and duration was indicated by combined reconstructions of

693 SST and mixed layer temperatures from the subarctic Pacific (Riethdorf et al., 2013).  
694 At that time, the rising eustatic sea level (Spratt and Lisiecki, 2016) would have  
695 supported the intrusion of Alaska Stream into the Bering Sea by deepening and  
696 opening glacial closed straits of the Aleutian Islands chain, while reducing the  
697 advection of the Alaska Stream to the subarctic Pacific gyre (Riethdorf et al., 2013).  
698 In this scenario, saltier and more stratified surface water conditions would have  
699 inhibited brine rejection and subsequent formation and ventilation of NPIW (Lam et  
700 al., 2013), leading to a reorganization of the Pacific water mass, closely coupled to the  
701 collapse and resumption modes of the AMOC during these two intervals.

#### 702 **6.4 Increased storage of CO<sub>2</sub> at mid-depth water in the North Pacific at the B/A**

703 One of the striking features of RSEs data is higher Mo/Mn ratios and excess U  
704 concentrations across the B/A, supporting an expansion of Oxygen Minimum Zone in  
705 the North Pacific (Galbraith and Jaccard, 2015; Jaccard and Galbraith, 2012; Moffitt  
706 et al., 2015) and coinciding with the termination of atmospheric CO<sub>2</sub> concentration  
707 rise (Marcott et al., 2014) (Figure 7e). As described above, it can be related to the  
708 upwelling of nutrient- and CO<sub>2</sub>-rich Pacific Deep Water due to resumption of AMOC  
709 and enhanced export production. Notably, boron isotope data measured on  
710 surface-dwelling foraminifera in core MD01-2416 situated in the western subarctic  
711 North Pacific did reveal a decrease in near-surface pH and an increase in pCO<sub>2</sub> at the  
712 onset of B/A (Gray et al., 2018), indicating that the subarctic North Pacific is a source  
713 of relatively high atmospheric CO<sub>2</sub> concentration at that time. Here we cannot  
714 conclude that the same processes could have occurred in the subtropical North Pacific  
715 due to the lack of well-known drivers to draw out of the old carbon in the deep sea  
716 into the atmosphere. In combination with published records from the North Pacific  
717 (Addison et al., 2012; Cartapanis et al., 2011; Crusius et al., 2004; Galbraith et al.,  
718 2007; Lembke-Jene et al., 2017; Shibahara et al., 2007), an expansion of  
719 oxygen-depletion zone during the B/A suggest an increase in respired carbon storage  
720 at mid-depth waters of the North Pacific, which likely stalls the rise of atmospheric  
721 CO<sub>2</sub>. Our results support the findings by Galbraith et al. (2007). Given the sizeable  
722 volume of the North Pacific, potentially, once the respired carbon could be emitted to

723 the atmosphere in stages, which would bring the planet out of the last ice age (Jaccard  
724 and Galbraith, 2018).

## 725 **7. Conclusions**

726 Our geochemical results of sediment core CSH1 revealed substantial changes in  
727 intermediate water redox conditions in the northern Okinawa Trough over the last 50  
728 ka on orbital and millennial timescales. Enhanced sedimentary oxygenation mainly  
729 occurred during cold intervals, such as the last glacial period, Heinrich stadials 1 and  
730 2, and during the middle and late Holocene, while diminished sedimentary  
731 oxygenation prevailed during the Bölling-Alleröd and Preboreal. The sedimentary  
732 oxygenation variability presented here provides key evidence for the substantial  
733 impact of ventilation of NPIW on the sedimentary oxygenation in the subtropical  
734 North Pacific and shows out-of-phase pattern with North Atlantic Climate during the  
735 last deglaciation. The linkage is attributable to the disruption of NPIW formation  
736 caused by climate changes in the North Atlantic, which is transferred to the North  
737 Pacific via atmospheric and oceanic teleconnections. We also suggest an expansion of  
738 oxygen-depleted zone and accumulation of respired carbon at the mid-depth waters  
739 from previously reported subarctic locations into the western subtropical the North  
740 Pacific during the B/A, coinciding with the termination of atmospheric CO<sub>2</sub> rise. A  
741 step-wise injection of such respired carbon into the atmosphere would be helpful to  
742 maintain high atmospheric CO<sub>2</sub> levels during the deglaciation and bring the planet out  
743 of the last ice age.

744

745 **Data availability.** All raw data are available to all interested researchers upon request.

746

747 **Author Contributions.** J.J.Z. and X.F.S. conceived the study. A.M.Z. performed  
748 geochemical analyses of bulk sediments. J.J.Z., X.F.S. K.S. and X.G. led the write up  
749 of the manuscript. All other authors provided comments on the manuscript and  
750 contributed to the final version of the manuscript.

751

752 **Competing interests:** The authors declare no competing interests.

753

754 **Acknowledgements**

755 Financial support was provided by the National Program on Global Change and  
756 Air-Sea Interaction (GASI-GEOGE-04), by the National Natural Science Foundation  
757 of China (Grant Nos.: 41476056, 41876065, 41420104005, 41206059, and U1606401)  
758 and by the Basic Scientific Fund for National Public Research Institutes of China  
759 (No.2016Q09) and International Cooperative Projects in Polar Study (201613) and  
760 Taishan Scholars Program of Shandong. This study is a contribution to the bilateral  
761 Sino-German collaboration project (funding through BMBF grant 03F0704A –  
762 SIGEPAX). XG, LLJ, GL, RT thank the bilateral Sino-German collaboration  
763 NOPAWAC project (BMBF grant No. 03F0785A).LLJ and RT acknowledge financial  
764 support through the national Helmholtz REKLIM Initiative. We would like to thank  
765 the anonymous reviewers, who helped to improve the quality of this manuscript. The  
766 data used in this study are available from the authors upon request  
767 (zoujianjun@fio.org.cn).

768

769 **References**

770 Addison, J. A., Finney, B. P., Dean, W. E., Davies, M. H., Mix, A. C., Stoner, J. S., and Jaeger, J.  
771 M.: Productivity and sedimentary  $\delta^{15}\text{N}$  variability for the last 17,000 years along the northern Gulf  
772 of Alaska continental slope, *Paleoceanography*, 27, PA1206, doi:1210.1029/2011PA002161, 2012.  
773 Algeo, T. J.: Can marine anoxic events draw down the trace element inventory of seawater?,  
774 *Geology*, 32, 1057-1060, 2004.  
775 Algeo, T. J. and Lyons, T. W.: Mo-total organic carbon covariation in modern anoxic marine  
776 environments: Implications for analysis of paleoredox and paleohydrographic conditions,  
777 *Paleoceanography*, 21, PA1016, doi: 1010.1029/2004pa001112, 2006.  
778 Algeo, T. J. and Tribouillard, N.: Environmental analysis of paleoceanographic systems based on  
779 molybdenum–uranium covariation, *Chemical Geology*, 268, 211-225, 2009.  
780 Andres, M., Jan, S., Sanford, T. B., Mensah, V., Centurioni, L. R., and Book, J. W.: Mean structure  
781 and variability of the Kuroshio from northeastern Taiwan to southwestern Japan, *Oceanography*,  
782 26, 84–95, 2015.  
783 Böhm, E., Lippold, J., Gutjahr, M., Frank, M., Blaser, P., Antz, B., Fohlmeister, J., Frank, N.,  
784 Andersen, M. B., and Deininger, M.: Strong and deep Atlantic meridional overturning circulation  
785 during the last glacial cycle, *Nature*, 517, 73-76, 2015.  
786 Barker, S., Knorr, G., Vautravers, M. J., Diz, P., and Skinner, L. C.: Extreme deepening of the  
787 Atlantic overturning circulation during deglaciation, *Nature Geoscience*, 3, 567-571, 2010.  
788 Beny, F., Toucanne, S., Skonieczny, C., Bayon, G., and Ziegler, M.: Geochemical provenance of



789 sediments from the northern East China Sea document a gradual migration of the Asian Monsoon  
790 belt over the past 400,000 years, *Quaternary Science Reviews*, 190, 161-175, 2018.

791 Bianchi, D., Dunne, J. P., Sarmiento, J. L., and Galbraith, E. D.: Data-based estimates of suboxia,  
792 denitrification, and N<sub>2</sub>O production in the ocean and their sensitivities to dissolved O<sub>2</sub>, *Global*  
793 *Biogeochemical Cycles*, 26, doi:10.1029/2011gb004209, 2012.

794 Brewer, P. G. and Peltzer, E. T.: Ocean chemistry, ocean warming, and emerging hypoxia:  
795 Commentary, *Journal of Geophysical Research: Oceans*, 121, 3659-3667, 2016.

796 Burdige, D. J.: The biogeochemistry of manganese and iron reduction in marine sediments,  
797 *Earth-Science Reviews*, 35, 249-284, 1993.

798 Cannariato, K. G. and Kennett, J. P.: Climatically related millennial-scale fluctuations in strength  
799 of California margin oxygen-minimum zone during the past 60 k.y, *Geology*, 27, 975-978, 1999.

800 Cartapanis, O., Tachikawa, K., and Bard, E.: Northeastern Pacific oxygen minimum zone  
801 variability over the past 70 kyr: Impact of biological production and oceanic ventilation,  
802 *Paleoceanography*, 26, PA4208, doi: 4210.1029/2011PA002126, 2011.

803 Cavalieri, D. J. and Parkinson, C. L.: On the relationship between atmospheric circulation and the  
804 fluctuations in the sea ice extents of the bering and okhotsk seas, *Journal of Geophysical*  
805 *Research-Oceans*, 92, 7141-7162, 1987.

806 Chang, A. S., Pedersen, T. F., and Hendy, I. L.: Effects of productivity, glaciation, and ventilation  
807 on late Quaternary sedimentary redox and trace element accumulation on the Vancouver Island  
808 margin, western Canada, *Paleoceanography*, 29, doi: 10.1002/2013PA002581, 2014.

809 Chang, Y.-P., Chen, M.-T., Yokoyama, Y., Matsuzaki, H., Thompson, W. G., Kao, S.-J., and  
810 Kawahata, H.: Monsoon hydrography and productivity changes in the East China Sea during the  
811 past 100,000 years: Okinawa Trough evidence (MD012404), *Paleoceanography*, 24, PA3208, doi:  
812 3210.1029/2007PA001577, 2009.

813 Chen, J., Zhang, D., Zhang, W., and Li, T.: The paleoclimatic change since the last glacialiation in  
814 the north of Okinawa Trough based on the spore-pollen records, *Acta Oceanologica Sinica*, 28,  
815 85-91, 2006 (in Chinese with English Abstract).

816 Cheng, H., Edwards, R. L., Sinha, A., Spötl, C., Yi, L., Chen, S., Kelly, M., Kathayat, G., Wang,  
817 X., Li, X., Kong, X., Wang, Y., Ning, Y., and Zhang, H.: The Asian monsoon over the past 640,000  
818 years and ice age terminations, *Nature*, 534, 640-646, 2016.

819 Cheng, H., Edwards, R. L., Southon, J., Matsumoto, K., Feinberg, J. M., Sinha, A., Zhou, W., Li,  
820 H., Li, X., Xu, Y., Chen, S., Tan, M., Wang, Q., Wang, Y., and Ning, Y.: Atmospheric 14C/12C  
821 changes during the last glacial period from Hulu Cave, *Science*, 362, 1293-1297, 2018.

822 Chikamoto, M. O., Menviel, L., Abe-Ouchi, A., Ohgaito, R., Timmermann, A., Okazaki, Y.,  
823 Harada, N., Oka, A., and Mouchet, A.: Variability in North Pacific intermediate and deep water  
824 ventilation during Heinrich events in two coupled climate models, *Deep Sea Research Part II:*  
825 *Topical Studies in Oceanography*, 61-64, 114-126, 2012.

826 Clark, P. U., Shakun, J. D., Baker, P. A., Bartlein, P. J., Brewer, S., Brook, E., Carlson, A. E.,  
827 Cheng, H., Kaufman, D. S., Liu, Z., Marchitto, T. M., Mix, A. C., Morrill, C., Otto-Bliesner, B. L.,  
828 Pahnke, K., Russell, J. M., Whitlock, C., Adkins, J. F., Blois, J. L., Clark, J., Colman, S. M., Curry,  
829 W. B., Flower, B. P., He, F., Johnson, T. C., Lynch-Stieglitz, J., Markgraf, V., McManus, J.,  
830 Mitrovica, J. X., Moreno, P. I., and Williams, J. W.: Global climate evolution during the last  
831 deglaciation, *Proceedings of the National Academy of Sciences of the United States of America*,  
832 109, E1134-E1142, 2012.

833 Clemens, S. C., Holbourn, A., Kubota, Y., Lee, K. E., Liu, Z., Chen, G., Nelson, A., and  
834 Fox-Kemper, B.: Precession-band variance missing from East Asian monsoon runoff, *Nature*  
835 *Communications*, 9, 3364, doi: 3310.1038/s41467-41018-05814-41460, 2018.

836 Crusius, J., Calvert, S., Pedersen, T., and Sage, D.: Rhenium and molybdenum enrichments in  
837 sediments as indicators of oxic, suboxic and sulfidic conditions of deposition, *Earth and Planetary*  
838 *Science Letters*, 145, 65-78, 1996.

839 Crusius, J., Pedersen, T. F., Kienast, S., Keigwin, L., and Labeyrie, L.: Influence of northwest  
840 Pacific productivity on North Pacific Intermediate Water oxygen concentrations during the  
841 Boiling-Allerod interval (14.7-12.9 ka), *Geology*, 32, 633-636, 2004.

842 Dahl, T. W., Anbar, A. D., Gordon, G. W., Rosing, M. T., Frei, R., and Canfield, D. E.: The  
843 behavior of molybdenum and its isotopes across the chemocline and in the sediments of sulfidic  
844 Lake Cadagno, Switzerland, *Geochimica et Cosmochimica Acta*, 74, 144-163, 2010.

845 Dean, W. E., Gardner, J. V., and Piper, D. Z.: Inorganic geochemical indicators of  
846 glacial-interglacial changes in productivity and anoxia on the California continental margin,  
847 *Geochimica et Cosmochimica Acta*, 61, 4507-4518, 1997.

848 Delcroix, T. and Murtugudde, R.: Sea surface salinity changes in the East China Sea during  
849 1997–2001: Influence of the Yangtze River, *Journal of Geophysical Research: Oceans*, 107, 8008,  
850 doi:8010.1029/2001JC000893, 2002.

851 Dou, Y., Yang, S., Li, C., Shi, X., Liu, J., and Bi, L.: Deepwater redox changes in the southern  
852 Okinawa Trough since the last glacial maximum, *Progress in Oceanography*, 135, 77-90, 2015.

853 Emile-Geay, J., Cane, M. A., Naik, N., Seager, R., Clement, A. C., and van Geen, A.: Warren  
854 revisited: Atmospheric freshwater fluxes and “Why is no deep water formed in the North Pacific”,  
855 *Journal of Geophysical Research: Oceans*, 108, doi:10.1029/2001JC001058, 2003.

856 Freeman, E., Skinner, L. C., Tisserand, A., Dokken, T., Timmermann, A., Menviel, L., and  
857 Friedrich, T.: An Atlantic–Pacific ventilation seesaw across the last deglaciation, *Earth and*  
858 *Planetary Science Letters*, 424, 237-244, 2015.

859 Galbraith, E. D. and Jaccard, S. L.: Deglacial weakening of the oceanic soft tissue pump: global  
860 constraints from sedimentary nitrogen isotopes and oxygenation proxies, *Quaternary Science*  
861 *Reviews*, 109, 38-48, 2015.

862 Galbraith, E. D., Jaccard, S. L., Pedersen, T. F., Sigman, D. M., Haug, G. H., Cook, M., Southon, J.  
863 R., and Francois, R.: Carbon dioxide release from the North Pacific abyss during the last  
864 deglaciation, *Nature*, 449, 890-893, 2007.

865 Galbraith, E. D., Kienast, M., Pedersen, T. F., and Calvert, S. E.: Glacial-interglacial modulation  
866 of the marine nitrogen cycle by high-latitude O<sub>2</sub> supply to the global thermocline,  
867 *Paleoceanography*, 19, PA4007, doi:4010.1029/2003PA001000, 2004.

868 Ge, S., Shi, X., Wu, Y., Lee, T., Xiong, Y., and Saito, Y.: Rock magnetic property of gravity core  
869 CSH1 from the northern Okinawa Trough and the effect of early diagenesis, *Acta Oceanologica*  
870 *Sinica*, 26, 54-65, 2007.

871 Gong, X., Lembke-Jene, L., Lohmann, G., Knorr, G., Tiedemann, R., Zou, J. J., and Shi, X. F.:  
872 Enhanced North Pacific deep-ocean stratification by stronger intermediate water formation during  
873 Heinrich Stadial 1, *Nature Communications*, 10, 656, doi:610.1038/s41467-41019-08606-41462,  
874 2019.

875 Gray, W. R., Rae, J. W. B., Wills, R. C. J., Shevenell, A. E., Taylor, B., Burke, A., Foster, G. L.,  
876 and Lear, C. H.: Deglacial upwelling, productivity and CO<sub>2</sub> outgassing in the North Pacific Ocean,

877 Nature Geoscience, 11, 340-344, 2018.

878 Helz, G. R., Miller, C. V., Charnock, J. M., Mosselmans, J. F. W., Patrick, R. A. D., Garner, C. D.,  
879 and Vaughan, D. J.: Mechanism of molybdenum removal from the sea and its concentration in  
880 black shales: EXAFS evidence, *Geochimica et Cosmochimica Acta*, 60, 3631-3642, 1996.

881 Hofmann, A. F., Peltzer, E. T., Walz, P. M., and Brewer, P. G.: Hypoxia by degrees: Establishing  
882 definitions for a changing ocean, *Deep Sea Research Part I: Oceanographic Research Papers*, 58,  
883 1212-1226, 2011.

884 Hoogakker, B. A. A., Elderfield, H., Schmiedl, G., McCave, I. N., and Rickaby, R. E. M.:  
885 Glacial–interglacial changes in bottom-water oxygen content on the Portuguese margin, *Nature*  
886 *Geoscience*, 8, 40-43, 2015.

887 Horikawa, K., Asahara, Y., Yamamoto, K., and Okazaki, Y.: Intermediate water formation in the  
888 Bering Sea during glacial periods: Evidence from neodymium isotope ratios, *Geology*, 38,  
889 435-438, 2010.

890 Ichikawa, H. and Beardsley, R. C.: The Current System in the Yellow and East China Seas, *Journal*  
891 *of Oceanography*, 58, 77-92, 2002.

892 Itaki, T., Khim, B. K., and Ikehara, K.: Last glacial-Holocene water structure in the southwestern  
893 Okhotsk Sea inferred from radiolarian assemblages, *Marine Micropaleontology*, 67, 191-215,  
894 2008.

895 Itaki, T., Kim, S., Rella, S. F., Uchida, M., Tada, R., and Khim, B. K.: Millennial-scale variations  
896 of late Pleistocene radiolarian assemblages in the Bering Sea related to environments in shallow  
897 and deep waters, *Deep-Sea Research Part II-Topical Studies in Oceanography*, 61-64, 127-144,  
898 2012.

899 Ivanochko, T. S. and Pedersen, T. F.: Determining the influences of Late Quaternary ventilation  
900 and productivity variations on Santa Barbara Basin sedimentary oxygenation: a multi-proxy  
901 approach, *Quaternary Science Reviews*, 23, 467-480, 2004.

902 Jaccard, S. L. and Galbraith, E. D.: Direct ventilation of the North Pacific did not reach the deep  
903 ocean during the last deglaciation, *Geophysical Research Letters*, 40, 199-203, 2013.

904 Jaccard, S. L. and Galbraith, E. D.: Large climate-driven changes of oceanic oxygen  
905 concentrations during the last deglaciation, *Nature Geoscience*, 5, 151-156, 2012.

906 Jaccard, S. L. and Galbraith, E. D.: Push from the Pacific, *Nature Geoscience*, 11, 299-300, 2018.

907 Jaccard, S. L., Galbraith, E. D., Martínez-García, A., and Anderson, R. F.: Covariation of deep  
908 Southern Ocean oxygenation and atmospheric CO<sub>2</sub> through the last ice age, *Nature*, 530, 207-210,  
909 2016.

910 Jaccard, S. L., Galbraith, E. D., Sigman, D. M., Haug, G. H., Francois, R., Pedersen, T. F., Dulski,  
911 P., and Thierstein, H. R.: Subarctic Pacific evidence for a glacial deepening of the oceanic respired  
912 carbon pool, *Earth and Planetary Science Letters*, 277, 156-165, 2009.

913 Jian, Z. M., Chen, R. H., and Li, B. H.: Deep-sea benthic foraminiferal record of the  
914 paleoceanography in the southern Okinawa trough over the last 20000 years, *Science in China*  
915 *Series D-Earth Sciences*, 39, 551-560, 1996.

916 Kao, S. J., Horng, C. S., Hsu, S. C., Wei, K. Y., Chen, J., and Lin, Y. S.: Enhanced deepwater  
917 circulation and shift of sedimentary organic matter oxidation pathway in the Okinawa Trough  
918 since the Holocene, *Geophysical Research Letters*, 32, L15609, doi:15610.11029/12005GL023139,  
919 2005.

920 Kao, S. J., Liu, K. K., Hsu, S. C., Chang, Y. P., and Dai, M. H.: North Pacific-wide spreading of

921 isotopically heavy nitrogen during the last deglaciation: Evidence from the western Pacific,  
922 *Biogeosciences*, 5, 1641-1650, 2008.

923 Kao, S. J., Wu, C.-R., Hsin, Y.-C., and Dai, M.: Effects of sea level change on the upstream  
924 Kuroshio Current through the Okinawa Trough, *Geophysical Research Letters*, 33, L16604,  
925 doi:10.1029/2006gl026822, 2006.

926 Keigwin, L. D.: Glacial-age hydrography of the far northwest Pacific Ocean, *Paleoceanography*,  
927 13, 323-339, 1998.

928 Kim, S., Khim, B. K., Uchida, M., Itaki, T., and Tada, R.: Millennial-scale paleoceanographic  
929 events and implication for the intermediate-water ventilation in the northern slope area of the  
930 Bering Sea during the last 71 kyrs, *Global and Planetary Change*, 79, 89-98, 2011.

931 Klinkhammer, G. P. and Palmer, M. R.: Uranium in the oceans: Where it goes and why,  
932 *Geochimica et Cosmochimica Acta*, 55, 1799-1806, 1991.

933 Knorr, G. and Lohmann, G.: Rapid transitions in the Atlantic thermohaline circulation triggered by  
934 global warming and meltwater during the last deglaciation, *Geochemistry, Geophysics,*  
935 *Geosystems*, 8, DOI: 10.1029/2007gc001604, 2007.

936 Kohfeld, K. E. and Chase, Z.: Controls on deglacial changes in biogenic fluxes in the North  
937 Pacific Ocean, *Quaternary Science Reviews*, 30, 3350-3363, 2011.

938 Kubota, Y., Kimoto, K., Itaki, T., Yokoyama, Y., Miyairi, Y., and Matsuzaki, H.: Bottom water  
939 variability in the subtropical northwestern Pacific from 26 kyr BP to present based on Mg/Ca and  
940 stable carbon and oxygen isotopes of benthic foraminifera, *Climate of the Past*, 11, 803-824, 2015.

941 Kubota, Y., Kimoto, K., Tada, R., Oda, H., Yokoyama, Y., and Matsuzaki, H.: Variations of East  
942 Asian summer monsoon since the last deglaciation based on Mg/Ca and oxygen isotope of  
943 planktic foraminifera in the northern East China Sea, *Paleoceanography*, 25, PA4205,  
944 doi:10.1029/2009pa001891, 2010.

945 Lam, P. J., Robinson, L. F., Blusztajn, J., Li, C., Cook, M. S., McManus, J. F., and Keigwin, L. D.:  
946 Transient stratification as the cause of the North Pacific productivity spike during deglaciation,  
947 *Nature Geosci*, 6, 622-626, 2013.

948 Lee, K. E., Lee, H. J., Park, J.-H., Chang, Y.-P., Ikehara, K., Itaki, T., and Kwon, H. K.: Stability  
949 of the Kuroshio path with respect to glacial sea level lowering, *Geophysical Research Letters*, 40,  
950 392-396, doi:10.1029/2012gl051022, 2013.

951 Lembke-Jene, L., Tiedemann, R., Nürnberg, D., Kokfelt, U., Kozdon, R., Max, L., Röhl, U., and  
952 Gorbarenko, S. A.: Deglacial variability in Okhotsk Sea Intermediate Water ventilation and  
953 biogeochemistry: Implications for North Pacific nutrient supply and productivity, *Quaternary*  
954 *Science Reviews*, 160, 116-137, 2017.

955 Li, D., Zheng, L.-W., Jaccard, S. L., Fang, T.-H., Paytan, A., Zheng, X., Chang, Y.-P., and Kao,  
956 S.-J.: Millennial-scale ocean dynamics controlled export productivity in the subtropical North  
957 Pacific, *Geology*, 45, 651-654, 2017.

958 Li, T., Xu, Z., Lim, D., Chang, F., Wan, S., Jung, H., and Choi, J.: Sr-Nd isotopic constraints on  
959 detrital sediment provenance and paleoenvironmental change in the northern Okinawa Trough  
960 during the late Quaternary, *Palaeogeography, Palaeoclimatology, Palaeoecology*, 430, 74-84, 2015.

961 Li, T. G., Xiang, R., Sun, R. T., and Cao, Q. Y.: Benthic foraminifera and bottom water evolution  
962 in the middle-southern Okinawa Trough during the last 18 ka, *Science in China Series D-Earth*  
963 *Sciences*, 48, 805-814, 2005.

964 Li, Y. H. and Schoonmaker, J. E.: Chemical Composition and Mineralogy of Marine Sediments. In:

965 Treatise on Geochemistry (Second Edition), Turekian, K. K. (Ed.), Elsevier, Oxford, 2014.

966 Lim, D., Kim, J., Xu, Z., Jeong, K., and Jung, H.: New evidence for Kuroshio inflow and  
967 deepwater circulation in the Okinawa Trough, East China Sea: Sedimentary mercury variations  
968 over the last 20 kyr, *Paleoceanography*, 32, 571-579, 2017.

969 Liu, Y. H., Henderson, G. M., Hu, C. Y., Mason, A. J., Charnley, N., Johnson, K. R., and Xie, S. C.:  
970 Links between the East Asian monsoon and North Atlantic climate during the 8,200 year event,  
971 *Nature Geosci*, 6, 117-120, 2013.

972 Liu, Z., Otto-Bliesner, B. L., He, F., Brady, E. C., Tomas, R., Clark, P. U., Carlson, A. E.,  
973 Lynch-Stieglitz, J., Curry, W., Brook, E., Erickson, D., Jacob, R., Kutzbach, J., and Cheng, J.:  
974 Transient Simulation of Last Deglaciation with a New Mechanism for Bølling-Allerød Warming,  
975 *Science*, 325, 310-314, 2009.

976 Lohmann, G., Lembke-Jene, L., Tiedemann, R., Gong, X., Scholz, P., Zou, J., and Shi, X.:  
977 Challenges in the Paleoclimatic Evolution of the Arctic and Subarctic Pacific since the Last  
978 Glacial Period—The Sino–German Pacific–Arctic Experiment (SiGePAX), *Challenges*, 10, 13,  
979 doi:10.3390/challe10010013, 2019.

980 Lynch-Stieglitz, J.: The Atlantic Meridional Overturning Circulation and Abrupt Climate Change,  
981 *Annual Review of Marine Science*, 9, 83-104, 2017.

982 Lyons, T. W., Anbar, A. D., Severmann, S., Scott, C., and Gill, B. C.: Tracking Euxinia in the  
983 Ancient Ocean: A Multiproxy Perspective and Proterozoic Case Study, *Annual Review of Earth  
984 and Planetary Sciences*, 37, 507-534, 2009.

985 Machida, H.: The stratigraphy, chronology and distribution of distal marker-tephras in and around  
986 Japan, *Global and Planetary Change*, 21, 71-94, 1999.

987 Maithani, P. B. and Srinivasan, S.: Felsic Volcanic Rocks, a Potential Source of Uranium - An  
988 Indian Overview, *Energy Procedia*, 7, 163-168, 2011.

989 Marcott, S. A., Bauska, T. K., Buizert, C., Steig, E. J., Rosen, J. L., Cuffey, K. M., Fudge, T. J.,  
990 Severinghaus, J. P., Ahn, J., Kalk, M. L., McConnell, J. R., Sowers, T., Taylor, K. C., White, J. W.  
991 C., and Brook, E. J.: Centennial-scale changes in the global carbon cycle during the last  
992 deglaciation, *Nature*, 514, 616-619, 2014.

993 Matsumoto, K., Oba, T., Lynch-Stieglitz, J., and Yamamoto, H.: Interior hydrography and  
994 circulation of the glacial Pacific Ocean, *Quaternary Science Reviews*, 21, 1693-1704, 2002.

995 Max, L., Lembke-Jene, L., Riethdorf, J. R., Tiedemann, R., Nürnberg, D., Kuhn, H., and  
996 Mackensen, A.: Pulses of enhanced North Pacific Intermediate Water ventilation from the Okhotsk  
997 Sea and Bering Sea during the last deglaciation, *Climate of the Past*, 10, 591-605, 2014.

998 Max, L., Rippert, N., Lembke-Jene, L., Mackensen, A., Nürnberg, D., and Tiedemann, R.:  
999 Evidence for enhanced convection of North Pacific Intermediate Water to the low-latitude Pacific  
1000 under glacial conditions, *Paleoceanography*, 32, 41-55, 2017.

1001 McManus, J., Berelson, W. M., Klinkhammer, G. P., Hammond, D. E., and Holm, C.: Authigenic  
1002 uranium: Relationship to oxygen penetration depth and organic carbon rain, *Geochimica et  
1003 Cosmochimica Acta*, 69, 95-108, 2005.

1004 McManus, J. F., Francois, R., Gherardi, J. M., Keigwin, L. D., and Brown-Leger, S.: Collapse and  
1005 rapid resumption of Atlantic meridional circulation linked to deglacial climate changes, *Nature*,  
1006 428, 834-837, 2004.

1007 Menviel, L., England, M. H., Meissner, K. J., Mouchet, A., and Yu, J.: Atlantic-Pacific seesaw and  
1008 its role in outgassing CO<sub>2</sub> during Heinrich events, *Paleoceanography*, 29, 58-70, 2014.

1009 Moffitt, S. E., Moffitt, R. A., Sauthoff, W., Davis, C. V., Hewett, K., and Hill, T. M.:  
1010 Paleooceanographic Insights on Recent Oxygen Minimum Zone Expansion: Lessons for Modern  
1011 Oceanography, PLOS ONE, 10, e0115246, doi, 0115210.0111371/journal.pone.0115246, 2015.  
1012 Morford, J. L. and Emerson, S.: The geochemistry of redox sensitive trace metals in sediments,  
1013 *Geochimica et Cosmochimica Acta*, 63, 1735-1750, 1999.  
1014 Nakamura, H., Nishina, A., Liu, Z. J., Tanaka, F., Wimbush, M., and Park, J. H.: Intermediate and  
1015 deep water formation in the Okinawa Trough, *Journal of Geophysical Research-Oceans*, 118,  
1016 6881-6893, 2013.  
1017 Nameroff, T. J., Balistrieri, L. S., and Murray, J. W.: Suboxic trace metal geochemistry in the  
1018 Eastern Tropical North Pacific, *Geochimica et Cosmochimica Acta*, 66, 1139-1158, 2002.  
1019 Nameroff, T. J., Calvert, S. E., and Murray, J. W.: Glacial-interglacial variability in the eastern  
1020 tropical North Pacific oxygen minimum zone recorded by redox-sensitive trace metals,  
1021 *Paleoceanography*, 19, PA1010, doi:10.1029/2003PA000912, 2004.  
1022 Nishina, A., Nakamura, H., Park, J.-H., Hasegawa, D., Tanaka, Y., Seo, S., and Hibiya, T.: Deep  
1023 ventilation in the Okinawa Trough induced by Kerama Gap overflow, *Journal of Geophysical  
1024 Research: Oceans*, 121, 6092-6102, 2016.  
1025 Ohkushi, K., Hara, N., Ikehara, M., Uchida, M., and Ahagon, N.: Intensification of North Pacific  
1026 intermediate water ventilation during the Younger Dryas, *Geo-Mar Lett*, 36, 353-360, 2016.  
1027 Ohkushi, K., Itaki, T., and Nemoto, N.: Last Glacial-Holocene change in intermediate-water  
1028 ventilation in the Northwestern Pacific, *Quaternary Science Reviews*, 22, 1477-1484, 2003.  
1029 Ohkushi, K., Kennett, J. P., Zeleski, C. M., Moffitt, S. E., Hill, T. M., Robert, C., Beaufort, L., and  
1030 Behl, R. J.: Quantified intermediate water oxygenation history of the NE Pacific: A new benthic  
1031 foraminiferal record from Santa Barbara basin, *Paleoceanography*, 28, 453-467, 2013.  
1032 Okazaki, Y., Kimoto, K., Asahi, H., Sato, M., Nakamura, Y., and Harada, N.: Glacial to deglacial  
1033 ventilation and productivity changes in the southern Okhotsk Sea, *Palaeogeography  
1034 Palaeoclimatology Palaeoecology*, 395, 53-66, 2014.  
1035 Okazaki, Y., Sagawa, T., Asahi, H., Horikawa, K., and Onodera, J.: Ventilation changes in the  
1036 western North Pacific since the last glacial period, *Climate of the Past*, 8, 17-24, 2012.  
1037 Okazaki, Y., Seki, O., Nakatsuka, T., Sakamoto, T., Ikehara, M., and Takahashi, K.: *Cycladophora  
1038 davisiana* (Radiolaria) in the Okhotsk Sea: A key for reconstructing glacial ocean conditions,  
1039 *Journal of Oceanography*, 62, 639-648, 2006.  
1040 Okazaki, Y., Timmermann, A., Menviel, L., Harada, N., Abe-Ouchi, A., Chikamoto, M. O.,  
1041 Mouchet, A., and Asahi, H.: Deepwater Formation in the North Pacific During the Last Glacial  
1042 Termination, *Science*, 329, 200-204, 2010.  
1043 Okumura, Y. M., Deser, C., Hu, A., Timmermann, A., and Xie, S.-P.: North Pacific Climate  
1044 Response to Freshwater Forcing in the Subarctic North Atlantic: Oceanic and Atmospheric  
1045 Pathways, *Journal of Climate*, 22, 1424-1445, 2009.  
1046 Porter, S. C. and Zhisheng, A.: Correlation between climate events in the North Atlantic and China  
1047 during the last glaciation, *Nature*, 375, 305-308, 1995.  
1048 Praetorius, S. K., Mix, A. C., Walczak, M. H., Wolhowe, M. D., Addison, J. A., and Prah, F. G.:  
1049 North Pacific deglacial hypoxic events linked to abrupt ocean warming, *Nature*, 527, 362-366,  
1050 2015.  
1051 Qu, T. and Lukas, R.: The Bifurcation of the North Equatorial Current in the Pacific, *Journal of  
1052 Physical Oceanography*, 33, 5-18, 2003.

1053 Rühlemann, C., Müller, P. J., and Schneider, R. R.: Organic Carbon and Carbonate as  
1054 Paleoproductivity Proxies: Examples from High and Low Productivity Areas of the Tropical  
1055 Atlantic. In: Use of Proxies in Paleoceanography: Examples from the South Atlantic, Fischer, G.  
1056 and Wefer, G. (Eds.), Springer Berlin Heidelberg, Berlin, Heidelberg, 1999.

1057 Rae, J. W. B., Sarthein, M., Foster, G. L., Ridgwell, A., Grootes, P. M., and Elliott, T.: Deep  
1058 water formation in the North Pacific and deglacial CO<sub>2</sub> rise, *Paleoceanography*, 29, 645-667,  
1059 2014.

1060 Reimer, P. J., Bard, E., Bayliss, A., Beck, J. W., Blackwell, P. G., Bronk Ramsey, C., Buck, C. E.,  
1061 Cheng, H., Edwards, R. L., Friedrich, M., Grootes, P. M., Guilderson, T. P., Hafliðason, H., Hajdas,  
1062 I., Hatté, C., Heaton, T. J., Hoffmann, D. L., Hogg, A. G., Hughen, K. A., Kaiser, K. F., Kromer,  
1063 B., Manning, S. W., Niu, M., Reimer, R. W., Richards, D. A., Scott, E. M., Southon, J. R., Staff, R.  
1064 A., Turney, C. S. M., and van der Plicht, J.: IntCal13 and Marine13 Radiocarbon Age Calibration  
1065 Curves 0–50,000 Years cal BP, *Radiocarbon*, 55, 1869-1887, 2013.

1066 Rella, S. F., Tada, R., Nagashima, K., Ikehara, M., Itaki, T., Ohkushi, K., Sakamoto, T., Harada, N.,  
1067 and Uchida, M.: Abrupt changes of intermediate water properties on the northeastern slope of the  
1068 Bering Sea during the last glacial and deglacial period, *Paleoceanography*, 27, PA3203,  
1069 doi:3210.1029/2011pa002205, 2012.

1070 Riethdorf, J.-R., Max, L., Nuernberg, D., Lembke-Jene, L., and Tiedemann, R.: Deglacial  
1071 development of (sub) sea surface temperature and salinity in the subarctic northwest Pacific:  
1072 Implications for upper-ocean stratification, *Paleoceanography*, 28, doi:10.1002/palo.20014, 2013.

1073 Riethdorf, J.-R., Thibodeau, B., Ikehara, M., Nürnberg, D., Max, L., Tiedemann, R., and  
1074 Yokoyama, Y.: Surface nitrate utilization in the Bering sea since 180ka BP: Insight from  
1075 sedimentary nitrogen isotopes, *Deep Sea Research Part II: Topical Studies in Oceanography*,  
1076 125-126, 163-176, 2016.

1077 Rippert, N., Max, L., Mackensen, A., Cacho, I., Povea, P., and Tiedemann, R.: Alternating  
1078 Influence of Northern Versus Southern-Sourced Water Masses on the Equatorial Pacific  
1079 Subthermocline During the Past 240 ka, *Paleoceanography*, 32, 1256-1274, 2017.

1080 Rodríguez-Sanz, L., Mortyn, P. G., Herguera, J. C., and Zahn, R.: Hydrographic changes in the  
1081 tropical and extratropical Pacific during the last deglaciation, *Paleoceanography*, 28, 529-538,  
1082 2013.

1083 Saenko, O. A., Schmittner, A., and Weaver, A. J.: The Atlantic-Pacific seesaw, *Journal of Climate*,  
1084 17, 2033-2038, 2004.

1085 Sagawa, T. and Ikehara, K.: Intermediate water ventilation change in the subarctic northwest  
1086 Pacific during the last deglaciation, *Geophysical Research Letters*, 35, 5, doi:  
1087 10.1029/2008gl035133, 2008.

1088 Scott, C. and Lyons, T. W.: Contrasting molybdenum cycling and isotopic properties in euxinic  
1089 versus non-euxinic sediments and sedimentary rocks: Refining the paleoproxies, *Chemical  
1090 Geology*, 324–325, 19-27, 2012.

1091 Scott, C., Lyons, T. W., Bekker, A., Shen, Y., Poulton, S. W., Chu, X., and Anbar, A. D.: Tracing  
1092 the stepwise oxygenation of the Proterozoic ocean, *Nature*, 452, 456-459, 2008.

1093 Shao, H., Yang, S., Cai, F., Li, C., Liang, J., Li, Q., Hyun, S., Kao, S.-J., Dou, Y., Hu, B., Dong, G.,  
1094 and Wang, F.: Sources and burial of organic carbon in the middle Okinawa Trough during late  
1095 Quaternary paleoenvironmental change, *Deep Sea Research Part I: Oceanographic Research  
1096 Papers*, 118, 46-56, 2016.

1097 Shcherbina, A. Y., Talley, L. D., and Rudnick, D. L.: Direct observations of North Pacific  
1098 ventilation: Brine rejection in the Okhotsk Sea, *Science*, 302, 1952-1955, 2003.

1099 Shi, X., Wu, Y., Zou, J., Liu, Y., Ge, S., Zhao, M., Liu, J., Zhu, A., Meng, X., Yao, Z., and Han, Y.:  
1100 Multiproxy reconstruction for Kuroshio responses to northern hemispheric oceanic climate and the  
1101 Asian Monsoon since Marine Isotope Stage 5.1 (~88 ka), *Climate of the Past*, 10, 1735-1750,  
1102 2014.

1103 Shibahara, A., Ohkushi, K., Kennett, J. P., and Ikehara, K.: Late Quaternary changes in  
1104 intermediate water oxygenation and oxygen minimum zone, northern Japan: A benthic  
1105 foraminiferal perspective, *Paleoceanography*, 22, PA3213, doi:3210.1029/2005pa001234, 2007.

1106 Shimmiel, G. B. and Price, N. B.: The behaviour of molybdenum and manganese during early  
1107 sediment diagenesis — offshore Baja California, Mexico, *Marine Chemistry*, 19, 261-280, 1986.

1108 Sibuet, J. C., Letouzey, J., Barbier, F., Charvet, J., Foucher, J. P., Hilde, T. W. C., Kimura, M.,  
1109 Chiao, L.-Y., Marsset, B., Muller, C., and Stéphan, J. F.: Back Arc Extension in the Okinawa  
1110 Trough, *Journal of Geophysical Research: Solid Earth*, 92, 14041-14063, 1987.

1111 Sigman, D. M. and Boyle, E. A.: Glacial/interglacial variations in atmospheric carbon dioxide,  
1112 *Nature*, 407, 859-869, 2000.

1113 Spratt, R. M. and Lisiecki, L. E.: A Late Pleistocene sea level stack, *Clim. Past*, 12, 1079-1092,  
1114 2016.

1115 Sun, Y., Clemens, S. C., Morrill, C., Lin, X., Wang, X., and An, Z.: Influence of Atlantic  
1116 meridional overturning circulation on the East Asian winter monsoon, *Nature Geosci*, 5, 46-49,  
1117 2012.

1118 Sun, Y. B., Oppo, D. W., Xiang, R., Liu, W. G., and Gao, S.: Last deglaciation in the Okinawa  
1119 Trough: Subtropical northwest Pacific link to Northern Hemisphere and tropical climate,  
1120 *Paleoceanography*, 20, PA4005, doi:4010.1029/2004pa001061, 2005.

1121 Sundby, B., Martinez, P., and Gobeil, C.: Comparative geochemistry of cadmium, rhenium,  
1122 uranium, and molybdenum in continental margin sediments, *Geochimica et Cosmochimica Acta*,  
1123 68, 2485-2493, 2004.

1124 Talley, L. D.: Distribution foramtion of North Pacific Intermediate water, *Journal of Physical*  
1125 *Oceanography*, 23, 517-537, 1993.

1126 Talley, L. D.: Hydrographic Atlas of the World Ocean Circulation Experiment (WOCE). In:  
1127 Volume 2: Pacific Ocean, Sparrow, M., Chapman, P., and Gould, J. (Eds.), International WOCE  
1128 Project Office, Southampton, UK, 2007.

1129 Tribouillard, N., Algeo, T. J., Lyons, T., and Riboulleau, A.: Trace metals as paleoredox and  
1130 paleoproductivity proxies: An update, *Chemical Geology*, 232, 12-32, 2006.

1131 Ujiie, H. and Ujiie, Y.: Late Quaternary course changes of the Kuroshio Current in the Ryukyu Arc  
1132 region, northwestern Pacific Ocean, *Marine Micropaleontology*, 37, 23-40, 1999.

1133 Ujiie, Y., Asahi, H., Sagawa, T., and Bassinot, F.: Evolution of the North Pacific Subtropical Gyre  
1134 during the past 190 kyr through the interaction of the Kuroshio Current with the surface and  
1135 intermediate waters, *Paleoceanography*, 31, 1498-1513, 2016.

1136 Ujiie, Y., Ujiie, H., Taira, A., Nakamura, T., and Oguri, K.: Spatial and temporal variability of  
1137 surface water in the Kuroshio source region, Pacific Ocean, over the past 21,000 years: evidence  
1138 from planktonic foraminifera, *Marine Micropaleontology*, 49, 335-364, 2003.

1139 Vorlicek, T. P. and Helz, G. R.: Catalysis by mineral surfaces: Implications for Mo geochemistry  
1140 in anoxic environments, *Geochimica et Cosmochimica Acta*, 66, 3679-3692, 2002.



1141 Wahyudi and Minagawa, M.: Response of benthic foraminifera to organic carbon accumulation  
1142 rates in the Okinawa Trough, *Journal of Oceanography*, 53, 411-420, 1997.

1143 Wan, S. and Jian, Z.: Deep water exchanges between the South China Sea and the Pacific since the  
1144 last glacial period, *Paleoceanography*, 29, 1162-1178, 2014.

1145 Wang, Y., Cheng, H., Edwards, R. L., He, Y., Kong, X., An, Z., Wu, J., Kelly, M. J., Dykoski, C.  
1146 A., and Li, X.: The Holocene Asian Monsoon: Links to Solar Changes and North Atlantic Climate,  
1147 *Science*, 308, 854-857, 2005.

1148 Wu, Y., Cheng, Z., and Shi, X.: Stratigraphic and carbonate sediment characteristics of Core CSH1  
1149 from the northern Okinawa Trough, *Advances in Marine Science*, 22, 163-169, 2004 (in Chinese  
1150 with English Abstract).

1151 Wu, Y., Shi, X., Zou, J., Cheng, Z., Wang, K., Ge, S., and Shi, F.: Benthic foraminiferal  $\delta^{13}\text{C}$   
1152 minimum events in the southeastern Okhotsk Sea over the last 180ka, *Chinese Science Bulletin*,  
1153 59, 3066-3074, 2014.

1154 You, Y. Z.: The pathway and circulation of North Pacific Intermediate Water, *Geophysical*  
1155 *Research Letters*, 30, doi:10.1029/2003gl018561, 2003.

1156 You, Y. Z., Suginozono, N., Fukasawa, M., Yasuda, I., Kaneko, I., Yoritaka, H., and Kawamiya, M.:  
1157 Roles of the Okhotsk Sea and Gulf of Alaska in forming the North Pacific Intermediate Water,  
1158 *Journal of Geophysical Research-Oceans*, 105, 3253-3280, 2000.

1159 You, Y. Z., Suginozono, N., Fukasawa, M., Yoritaka, H., Mizuno, K., Kashino, Y., and Hartoyo, D.:  
1160 Transport of North Pacific Intermediate Water across Japanese WOCE sections, *Journal of*  
1161 *Geophysical Research-Oceans*, 108, doi: 10.1029/2002jc001662, 2003.

1162 Yu, H., Liu, Z. X., Berne, S., Jia, G. D., Xiong, Y. Q., Dickens, G. R., Wei, G. J., Shi, X. F., Liu, J.  
1163 P., and Chen, F. J.: Variations in temperature and salinity of the surface water above the middle  
1164 Okinawa Trough during the past 37 kyr, *Palaeogeography Palaeoclimatology Palaeoecology*, 281,  
1165 154-164, 2009.

1166 Zhang, X., Knorr, G., Lohmann, G., and Barker, S.: Abrupt North Atlantic circulation changes in  
1167 response to gradual CO<sub>2</sub> forcing in a glacial climate state, *Nature Geoscience*, 10, 518-524, 2017.

1168 Zhao, D., Wan, S., Toucanne, S., Clift, P. D., Tada, R., Révillon, S., Kubota, Y., Zheng, X., Yu, Z.,  
1169 Huang, J., Jiang, H., Xu, Z., Shi, X., and Li, A.: Distinct control mechanism of fine-grained  
1170 sediments from Yellow River and Kyushu supply in the northern Okinawa Trough since the last  
1171 glacial, *Geochemistry, Geophysics, Geosystems*, 18, 2949-2969, 2017.

1172 Zheng, X., Kao, S., Chen, Z., Menviel, L., Chen, H., Du, Y., Wan, S., Yan, H., Liu, Z., Zheng, L.,  
1173 Wang, S., Li, D., and Zhang, X.: Deepwater circulation variation in the South China Sea since the  
1174 Last Glacial Maximum, *Geophysical Research Letters*, 43, 8590-8599, 2016.

1175 Zheng, Y., Anderson, R., van Geen, A., and Fleisher, M.: Remobilization of authigenic uranium in  
1176 marine sediments by bioturbation, *Geochimica et Cosmochimica Acta*, 66, 1759-1772, 2002.

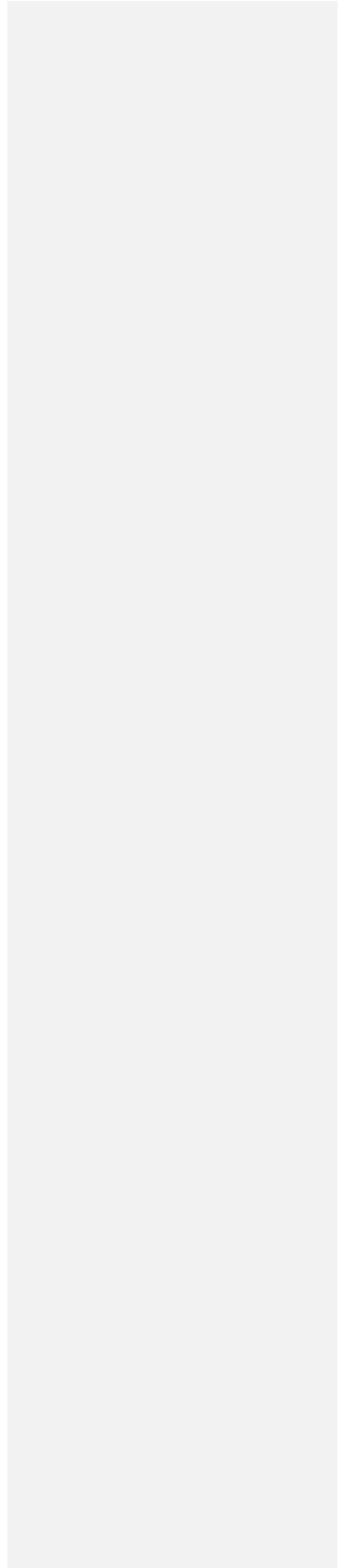
1177 Zheng, Y., Anderson, R., van Geen, A., and Kuwabara, J.: Authigenic molybdenum formation in  
1178 marine sediments: a link to pore water sulfide in the Santa Barbara Basin, *Geochimica et*  
1179 *Cosmochimica Acta*, 64, 4165-4178, 2000.

1180 Zhu, A., Shi, X., Zou, J., Wu, Y., Zhang, H., and Bai, Y.: Sediment Provenance and Fluxes in the  
1181 Northern Okinawa Trough During the last 88ka, *Marine Geology & Quaternary Geology*, 35, 1-8 ,  
1182 2015 (in Chinese with English Abstract).

1183 Zou, J., Shi, X., Liu, Y., Liu, J., Selvaraj, K., and Kao, S.-J.: Reconstruction of environmental  
1184 changes using a multi-proxy approach in the Ulleung Basin (Sea of Japan) over the last 48 ka,

1185 Journal of Quaternary Science, 27, 891-900, 2012.

1186



1187 **Captions**

1188 **Table 1.** Locations of different sediment core records and their source references  
1189 discussed in the text.

1190

1191 **Table 2.** Age control points adopted between planktic foraminifera species  
1192 *Globigerinoides ruber*  $\delta^{18}\text{O}$  of Core CSH1 and Chinese stalagmite  $\delta^{18}\text{O}$  (Cheng et al.,  
1193 2016) for tuning the age model between 10 ka and 60 ka in this study. A linear  
1194 interpolation was assumed between age control points.

1195

1196 **Figure 1.** (a) Spatial distribution of dissolved oxygen content at 700 m water depth in  
1197 the North Pacific. Black arrows denote simplified Kuroshio and Oyashio circulations  
1198 and North Pacific Intermediate Water (NPIW) in the North Pacific. The red thick  
1199 dashed line indicates transformation of Okhotsk Sea Intermediate Water (OSIW) by  
1200 cabbeling the subtropical NPIW along the subarctic-tropical frontal zone (You, 2003).  
1201 The light brown solid line with arrow indicates the spreading path of subtropical  
1202 NPIW from northeast North Pacific southward toward the low-latitude northwest  
1203 North Pacific (You, 2003). Yellow solid lines with arrow represent two passages  
1204 through which NPIW enter into the Okinawa Trough. This figure was created with  
1205 Ocean Data View (odv.awi.de). (b) Location of sediment core CSH1 investigated in  
1206 this study (red diamond). Also shown are locations of sediment cores PN-3, E017, 255  
1207 and MD012404 investigated previously from the Okinawa Trough, GH08-2004 from  
1208 the East of Ryukyu Island, GH02-1030 off the east of Japan, PC-23A from the Bering  
1209 Sea and ODP Site 1017 from the northeastern Pacific. Letters A to E represent the  
1210 sediment cores from and near the OT. The detailed information for these cores is  
1211 shown in Table 1.

1212

1213 **Figure 2.** Spatial distribution of sea surface salinity in the East China Sea. (a) summer  
1214 (July to September); (b) winter (January to March). Lower sea surface salinity in  
1215 summer relative to that of winter indicates strong effects of summer East Asian  
1216 Monsoon.

1217

1218 **Figure 3.** (a) Lithology and oxygen isotope ( $\delta^{18}\text{O}$ ) profile of planktic foraminifera  
1219 species *Globigerinoides ruber* (*G.ruber*) in core CSH1. (b) Plot of ages versus depth  
1220 for core CSH1. Three known ash layers are indicated by solid red rectangles. (c) Time  
1221 series of linear sedimentation rate (LSR) from core CSH1. (d) Comparison of age  
1222 model of core CSH1 with Chinese Stalagmite composite  $\delta^{18}\text{O}$  curve of (Cheng et al.,  
1223 2016). Tie points for CSH1 core chronology (Table 2) in Figures 3c and 3d are  
1224 designated by colored crosses.

1225

1226 **Figure 4.** Age versus (a)  $\text{CaCO}_3$  concentration, (b) Total nitrogen (TN) concentration,  
1227 (c) Total organic carbon (TOC) concentration, (d) C/N molar ratio, (e) linear  
1228 sedimentation rate (LSR), (f) Al concentration, (g) Mn concentration, (h) Mo/Mn ratio,  
1229 (i) Mo concentration, (j) excess Mo concentration, (k) U concentration and (l) excess  
1230 U concentration and (m)  $(\text{Mo}/\text{U})_{\text{excess}}$  ratio in core CSH1. Light gray and dark gray  
1231 vertical bars indicate different sediment intervals in core CSH1. 8.2 ka, PB, YD, B/A,  
1232 HS1, LGM and HS2 refer to 8,200 year cold event, Preboreal, Younger Dryas, Bölling  
1233 - Alleröd, Heinrich Stadial 1, Last Glacial Maximum and Heinrich Stadial 2,  
1234 respectively, which were identified in core CSH1. Blue solid diamonds in Figure 4m  
1235 indicate the age control points.

1236

1237 **Figure 5.** Scatter plots of  $\text{Mo}_{\text{excess}}$  vs Mn concentrations and  $\text{U}_{\text{excess}}$  concentration vs  
1238 Mo/Mn ratio at different time intervals in core CSH1. A various correlation is present  
1239 in core CSH1 at different time intervals, which shows their complicated geochemical  
1240 behaviors (Figs.5a and 5b). Strong positive correlation between Mo/Mn ratio and  
1241  $\text{U}_{\text{excess}}$  concentration (Fig.5c) suggest that Mo/Mn ratio is a reliable proxy to track  
1242 sedimentary redox conditions in the geological past.

1243

1244 **Figure 6.** Proxy-related reconstructions of mid-depth sedimentary oxygenation at site  
1245 CSH1 (this study) compared with oxygenation records from other locations of the  
1246 North Pacific and published climatic and environmental records from the Okinawa

1247 Trough. From top to bottom: (a) CaCO<sub>3</sub> concentration, (b) U<sub>excess</sub> concentration, (c)  
1248 Mo/Mn ratio, and (d) sea surface temperature (SST) (Shi et al., 2014), (e) abundance  
1249 of *P.obliquiloculata* in core CSH1 (Shi et al., 2014), (f) bulk sedimentary organic  
1250 matter δ<sup>15</sup>N in core MD01-2404 (Kao et al., 2008), (g) δ<sup>13</sup>C of epibenthic  
1251 foraminiferal *C.wuellerstorfi* in core PN-3 (Wahyudi and Minagawa, 1997), (h)  
1252 relative abundance of *B. aculeata* (hypoxia-indicating species) and (i) *C.hyalinea*  
1253 (oxygen-rich indicating species) (Li et al., 2005), (j) dysoxic taxa (%) in core ODP  
1254 167-1017 in the northeastern Pacific (Cannariato and Kennett, 1999) and (k) δ<sup>13</sup>C of  
1255 benthic foraminiferal *Uvigerina akitaensis* in core PC23A in the Bering Sea (Rella  
1256 et al., 2012). Light gray and dark gray vertical bars are the same as those in Figure 4.

1257

1258 **Figure 7.** Proxy records favoring the existence of out-of-phase connections between  
1259 the subtropical North Pacific and North Atlantic during the last deglaciation and  
1260 enhanced carbon storage at mid-depth waters. (a) U<sub>excess</sub> concentration in core CSH1;  
1261 (b) Mo/Mn ratio in core CSH1; (c) benthic δ<sup>13</sup>C record in core PC-23A in the Bering  
1262 Sea (Rella et al., 2012); (d) Indicator of strength of Atlantic Meridional Ocean  
1263 Circulation (<sup>231</sup>Pa/<sup>230</sup>Th) (Böhm et al., 2015; McManus et al., 2004); (e) Atmospheric  
1264 CO<sub>2</sub> concentration (Marcott et al., 2014). Light gray and dark gray vertical bars are  
1265 the same as those in Figure 4.

1266

Table 1

Label in Figure 1b	Station	Latitude (°N)	Longitude (°E)	Water depth (m)	Area	Reference
	CSH1	31.23	128.72	703	Okinawa Trough	this study
A	PN-3	28.10	127.34	1058	Okinawa Trough	Wahyudi and Minagawa, (1997)
B	MD012404	26.65	125.81	1397	Okinawa Trough	Kao et al., (2008)
C	E017	26.57	126.02	1826	Okinawa Trough	Li et al., (2005)
D	255	25.20	123.12	1575	Okinawa Trough	Jian et al., (1996)
E	GH08-2004	26.21	127.09	1166	East of Ryukyu Island	Kubota et al. (2015)
	GH02-1030	42.23	144.21	1212	Off Japan	Sagawa and Ikehara, (2008)
	PC-23A	60.16	179.46	1002	Bering Sea	Rella et al.,(2012)
	ODP Site1017	34.54	239.11	955	NE Pacific	Cannariato and Kennett, (1999)

1 Table 2

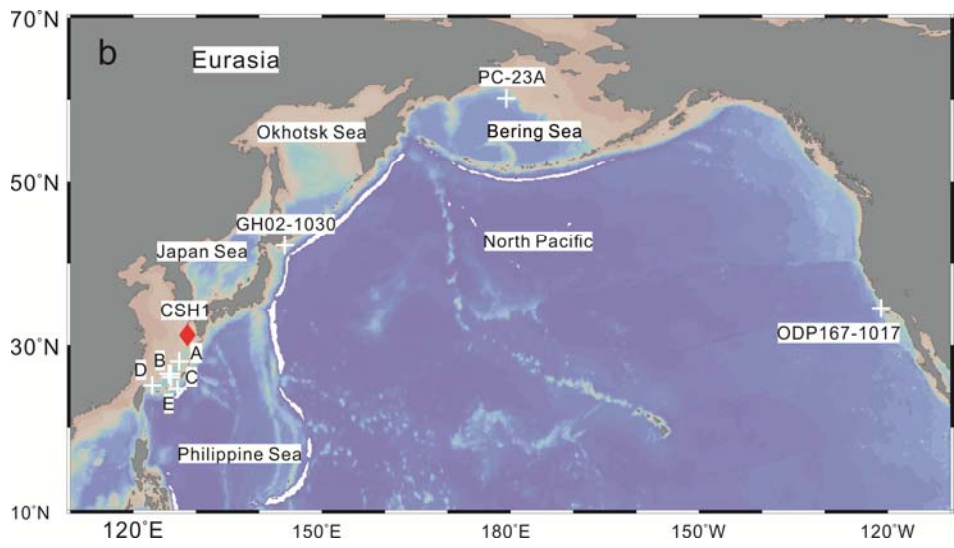
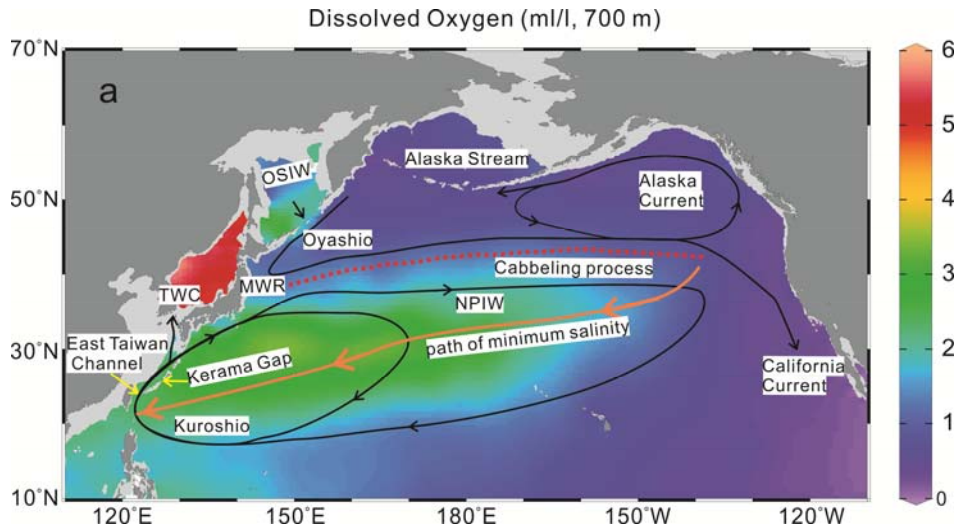
2

Depth(cm)	AMS <sup>14</sup> C (yr)	Error (yr)	Calibrated Age (yr)	Tie Point Type	LSR (cm/ka)	Source
10	3420	±35	3296	<sup>14</sup> C		Shi et al., (2014)
106	7060	± 40	7545	<sup>14</sup> C	22.59	Shi et al., (2014)
218			12352	Stalagmite, YD	23.30	This study
322			16029	Stalagmite, H1	28.28	This study
362			19838	Stalagmite	10.50	This study
506			24163	Stalagmite, H2	33.29	This study
698			28963	Stalagmite, DO4	40.00	This study
834			32442	Stalagmite, DO5	39.09	This study
938			37526	Stalagmite, DO8	20.46	This study
978			39468	Stalagmite, H4	20.60	This study
1058			46151	Stalagmite, DO12	11.97	This study
1122			49432	Stalagmite, DO13	19.51	This study
1242			52831	Stalagmite, DO14	35.30	This study
1282			57241	Stalagmite, DO16	9.07	This study
1346			61007	Stalagmite, H6	16.99	This study
1530		±2590	73910	MIS4/5	14.26	Shi et al., (2014)
1610		±3580	79250	MIS 5.1	14.98	Shi et al., (2014)

3

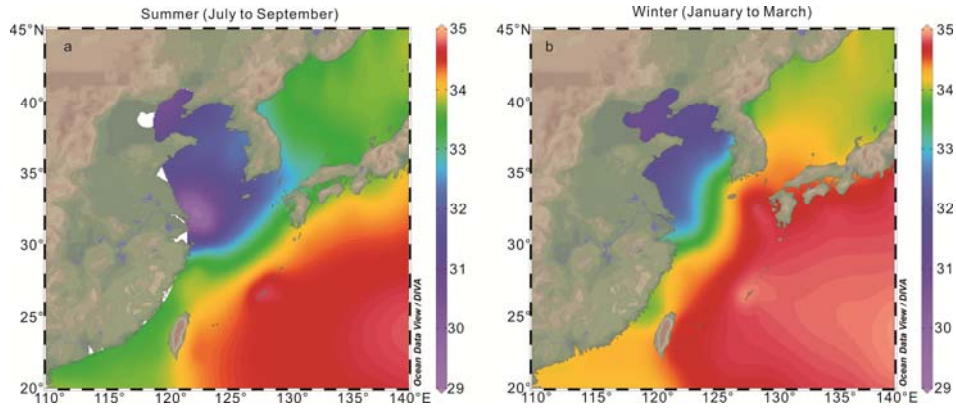
4

5 Fig.1





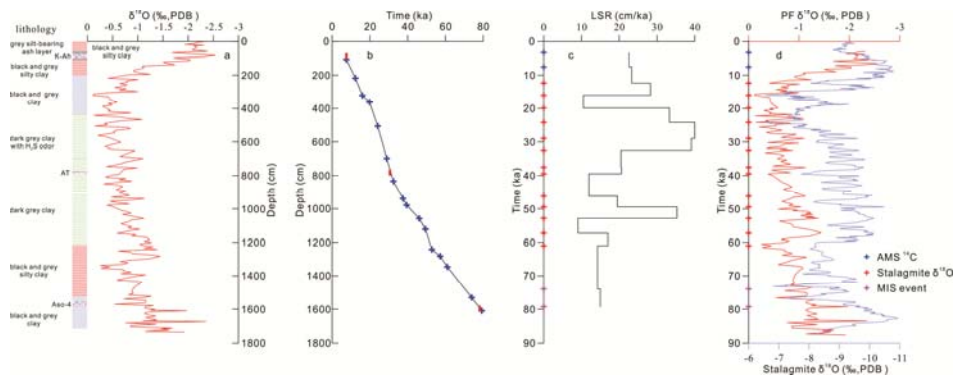
11 Fig.2



12

13

14 Fig.3

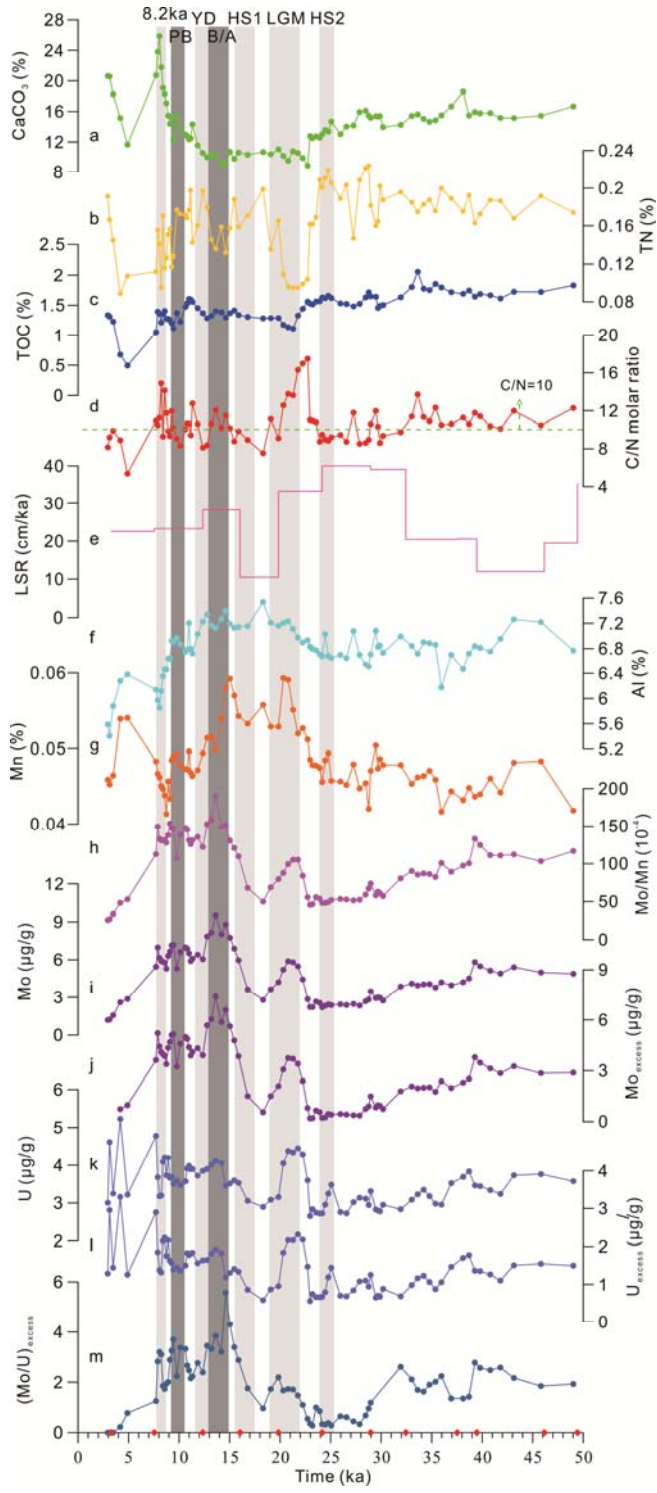


15

16

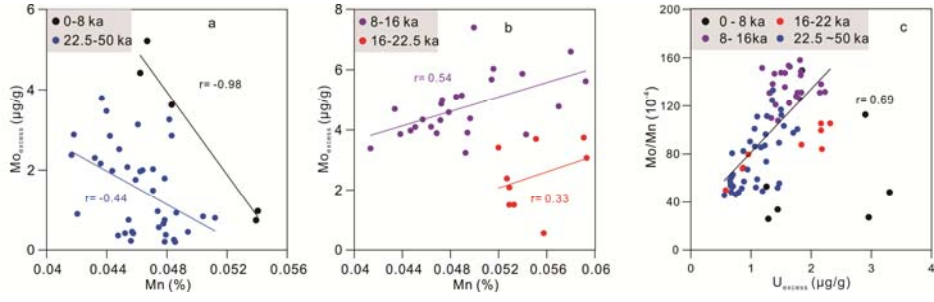
17

18 Fig.4



20 Fig.5

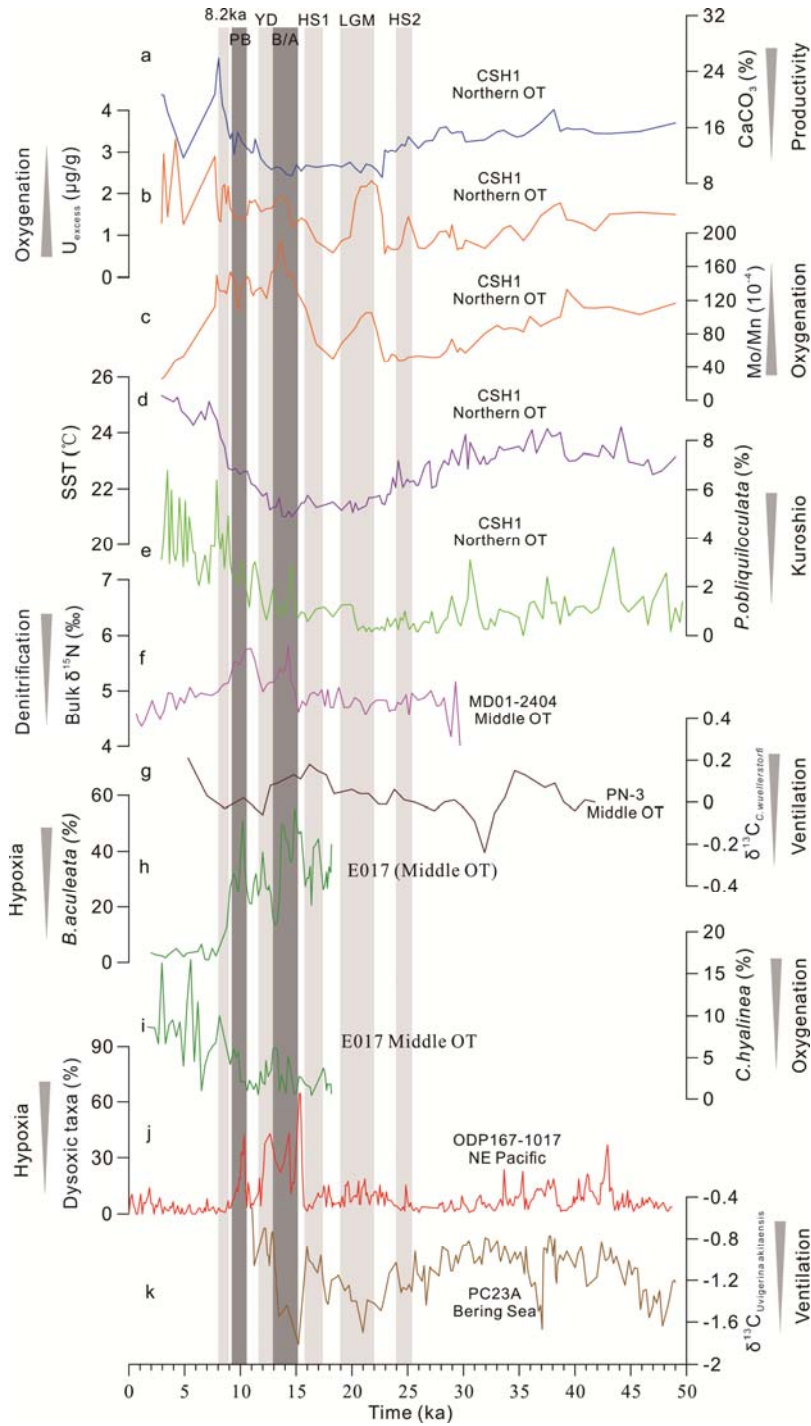
21



22

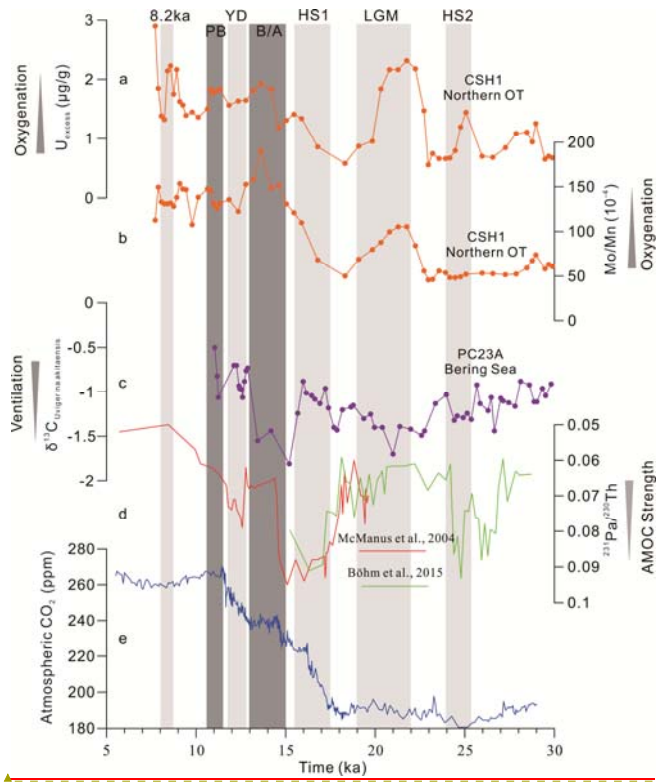
23

24 Fig.6



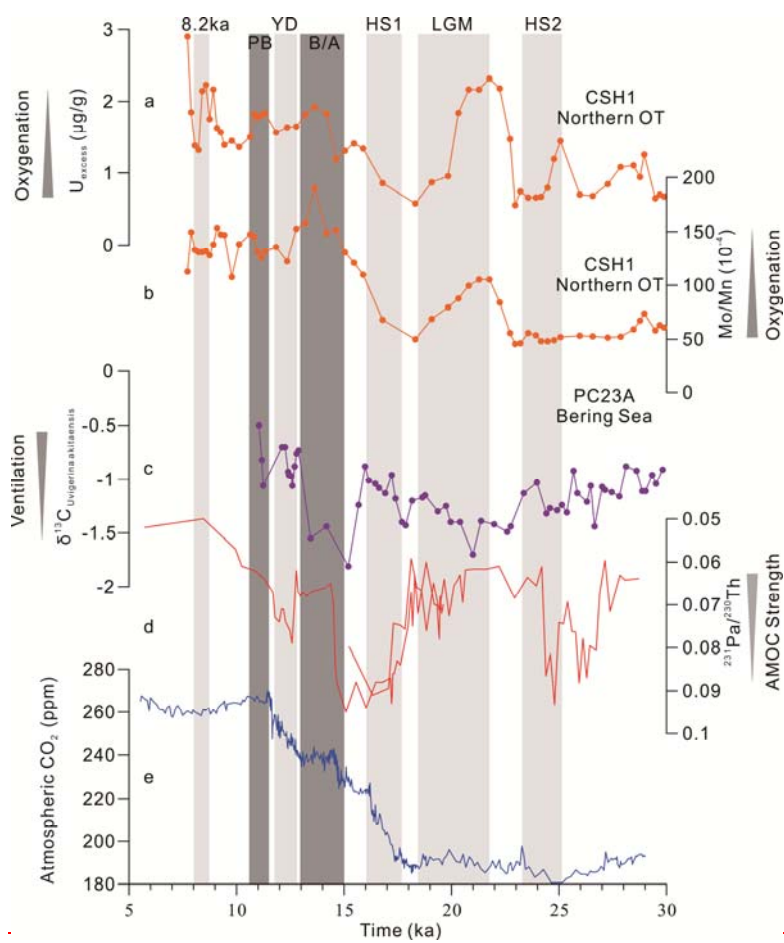
25  
26

27 Fig.7



28

带格式的: 字体: 小四



29

30